

The Combined Effects of Alzheimer's Disease, Stroke and Gender on A β Burden and Synaptic Density

Minou Verhaeg¹, Klara Lohkamp¹, Maximilian Wiesmann¹, Amanda Kiliaan¹

¹*Department of Neuroanatomy, Radboud University Medical Centre Nijmegen, Donders Institute for Brain, Cognition and Behaviour, The Netherlands*

Alzheimer's disease (AD) and stroke are both diseases that have a very high impact on the current society. Prevalence of both conditions is expected to rise due to the increasing life expectancy of the population. There is a close relation between stroke and AD (e.g., prevalence of stroke is increased in AD patients and stroke increases the risk of AD). In the current longitudinal study, the interaction of stroke and AD was investigated in the APP^{swE}/PS1^{dE9} mouse model with a 30 minute-induced middle cerebral artery occlusion in the right hemisphere. This study focused on the A β burden and synaptic density, via synaptophysin expression in the APP model, the stroke model and the combined APP/stroke model. Both male and female mice were used because there are differences in risk factors and pathology in both AD and stroke between the two sexes. An increased A β burden, especially visible in the cortex, hippocampus, thalamus and basal ganglia, combined with higher A β concentrations in the anterior part of the brain were observed in female compared to male APP mice. Eight months after stroke induction, male APP mice showed a lower A β burden in the cortex of the affected hemisphere compared to the unaffected hemisphere. Furthermore, between the hemispheres, asymmetrical expression of synaptophysin was observed in wildtype sham animals. Male mice had a higher synaptophysin expression in the affected hemisphere, while female mice had a decreased synaptophysin expression in the affected hemisphere. Lastly, female APP mice showed lower synaptophysin expression in the affected hemisphere than males. Overall, stroke affected the A β burden differently in male and female mice. These gender differences are most likely also the cause of the observed differences in synaptic density. More research into other AD markers, especially vascular pathology, is required to further determine the long-term effects of stroke on AD.

Keywords: Alzheimer's disease, ischemic stroke, neuropathology, animal models, amyloid beta, synaptic density

Corresponding author: Minou Verhaeg; E-mail: minou_verhaeg@hotmail.com

List of abbreviations

AD	Alzheimer's disease
APP	Amyloid beta precursor protein
A β	Amyloid beta
B2M	Beta-2 microglobulin
CAA	Cerebral amyloid angiopathy
CBF	Cerebral blood flow
CCA	Common carotid artery
CSF	Cerebral spinal fluid
ELISA	Enzyme-linked immune sorbent assay
EpoE	Epolipoprotein E
GLUT-1	Glucose transporter 1
IHC	Immunohistochemical staining
MCA	Middle cerebral artery
MCAO	Middle cerebral artery occlusion
MCI	Mild cognitive impairment
PBS	Phosphate-buffered saline
PSD-95	Post synaptic density marker 95
qPCR	Quantitative polymerase chain reaction
SPB	Systolic blood pressure
SYP	Synaptophysin
WT	Wildtype

Due to increasing life expectancy, dementia has developed into one of the major public health problems worldwide. In America alone it is estimated that 5.8 million people were living with Alzheimer's disease (AD) in 2019 (Association, 2019). AD is the most common form of dementia and starts with occasional problems with episodic memory, referred to as mild cognitive impairment (MCI). Ultimately MCI can develop into dementia with profound memory impairments, disorientation, and deficits in motor function (D. J. Selkoe & Schenk, 2003). From a neuropathological perspective AD is characterized by the accumulation of amyloid beta (A β) plaques, neurofibrillary tau tangles, and the loss of neurons and their synapses (Dennis J Selkoe, 2002). The cognitive decline observed in AD is most closely associated with the synaptic loss that is observed in the brain (Dennis J Selkoe, 2002). Hippocampus, amygdala and the frontal, temporal, and parietal lobes undergo significant synaptic loss (DeKosky S.T., 1996). Previous studies have found that a reduction in synaptic density (indicated by synaptophysin (SYP) expression), and overall synaptic degeneration play a critical role in the progression of AD (Robinson et al., 2014; Wuwongse et al., 2013; Zeng et al., 2015). This synaptic dysfunction, along with neuroinflammation, apoptosis, and dysregulation of neurons, is partially mediated by A β and tau proteins

(Goedert & Spillantini, 2006; Klyubin, Cullen, Hu, & Rowan, 2012; Shankar & Walsh, 2009).

The accumulated A β proteins (plaques) are another characteristic of AD. These plaques are specific to AD and are not present in other types of dementia, or directly linked to dementia symptoms (Jarrett, Berger, & Lansbury Jr, 1993). The A β protein is commonly present in two lengths: A β 40 and A β 42. A β 42 is more prone to aggregation, leading to the formation of the A β plaques (Jarrett et al., 1993). These protein aggregations are primarily present in the hippocampus, amygdala and cortices of the frontal, temporal and parietal lobes (Gouras et al., 2000; D. J. Selkoe & Schenk, 2003). AD can be divided into two types: familial and sporadic AD. Most AD patients have no genetic predisposition and are classified as sporadic. The smaller group, familial AD, is autosomal dominant and strikes most often before the age of 65. This familial variant of AD is driven by mutations in A β precursor protein (APP), apolipoprotein E (EpoE) or presenilin 1 or 2, which cause elevated levels of A β 40, A β 42 and the ratio between them (Cacace, Slegers, & Van Broeckhoven, 2016; Holtzman et al., 2000). One hypothesis, the A β hypothesis, states that A β deposits are also the causal factor in the sporadic form of AD. However, the A β hypothesis is under heavy debate, since A β does not directly cause dementia symptoms (de la Torre, 2004). Increasingly more evidence points to a direct involvement of the cerebral vasculature in the development of AD (de la Torre, 2004). Therefore, the vascular hypothesis was introduced, wherein vascular factors contribute significantly to the development of dementia and AD.

Vascular hypothesis

Multiple vascular factors have been proven to contribute to the risk of developing AD (R. Kalaria, 2002; R. N. Kalaria, Akinyemi, & Ihara, 2012). In total, 60 to 90% of AD patients show cerebrovascular pathology at autopsy (R. N. Kalaria et al., 2012). In the first documented case of AD in 1906 by Alois Alzheimer arteriosclerotic changes in cerebral blood vessels already were mentioned (Drouin & Drouin, 2017). Changes in cerebral vasculature are closely linked to AD and A β accumulation, since efflux transporters located in the cerebral vessels and drainage through perivascular pathways into the cervical lymph nodes are mainly responsible for the clearance of A β out of the brain (Ueno, Chiba, Matsumoto, Nakagawa, & Miyataka, 2014). A β deposits have also been observed

inside the blood vessels in the brain, known as a condition called cerebral amyloid angiopathy (CAA) (Lewis et al., 2006; McGowan et al., 2005). There is a significant association between certain vascular risk factors, such as hypertension in midlife, and development of AD or other forms of cognitive decline later in life (Kivipelto et al., 2001; Skoog et al., 1996). Hypertension leads to atherosclerotic changes in the arteries, lowering the cerebral blood flow (CBF) (Skoog et al., 1996). A lower CBF can cause ischemia, increases the production of A β and reduces A β clearance, leading to an overall higher concentration of A β in the brain (Nelson, Sweeney, Sagare, & Zlokovic, 2016; Ramanathan, Nelson, Sagare, & Zlokovic, 2015; Ueno et al., 2014). The onset of hypertension can already appear decades before the onset of AD (Skoog et al., 1996).

Ischemic stroke

Hypertension is also a major risk factor for further vascular complications, including stroke. Stroke can be divided into two types: ischemic stroke, in which an artery is occluded, and hemorrhagic stroke, in which an artery bursts (Amarenco, Bogousslavsky, Caplan, Donnan, & Hennerici, 2009). During a stroke, the CBF to the afferent brain areas of the affected vessels is severely lowered. Ischemic stroke is the most common variant, which most often occurs in a specific artery. Over 90% of ischemic stroke cases involve the middle cerebral artery (Roger et al., 2011). The affected area can be divided into an area of irreversible injury, the ischemic core, and an area of damaged but salvageable tissue, the penumbra. The penumbra is hypo-perfused, but cells still maintain basic cerebral metabolic rate and can be salvaged when reperfusion to the brain area occurs (Marchal et al., 1996). Due to the loss of CBF and the drop in clearance, accumulation of A β is seen in the regions directly affected by the stroke.

There is a clear link between AD and stroke. Stroke has been proven to double the prevalence of AD in elderly (Honig et al., 2003; Sun et al., 2006). Furthermore, AD patients with stroke seem to have more severe dementia compared to those who do not suffer from stroke (Leys et al., 1999; White et al., 2002), due to the tissue and vascular damage caused by the stroke. The interaction between vascularity, especially stroke, and AD pathology works both ways. A stroke does not only strengthen AD symptoms, but people with AD also have a high risk of suffering from a stroke (Chi, Chien, Ku, Hu, & Chiou, 2013). Stroke and AD also share a lot of the same risk factors such as aging (Sahathevan,

Brodthmann, & Donnan, 2012), hypertension, diabetes, hypercholesterolemia, smoking and obesity (de Bruijn & Ikram, 2014; Nelson et al., 2016). More and more studies start to question the clear diagnostic separation between vascular dementia and AD (Agüero-Torres, Kivipelto, & von Strauss, 2006; de la Torre, 2004). Due to the significant contribution of these vascular factors a model on the development of dementia was developed by Sweeney et al. (Fig. 1) (Sweeney, Sagare, & Zlokovic, 2015). This model takes both vascular damage and the contribution of A β into account. It also includes the interaction of the two factors, possibly through the interaction between stroke and APP, as this link has been proven in animal models (Jendroska, Hoffmann, & Patt, 1997; Jendroska et al., 1995; Nakamura, Takeda, Niigawa, Hariguchi, & Nishimura, 1992). The precise mechanism behind this interaction however, is still not well understood (de la Torre, 2004).

Gender differences

One highly significant risk factor which needs to be studied in more detail is the effect of gender. Both in AD and stroke sex differences play a profound role in prevalence and progression of the

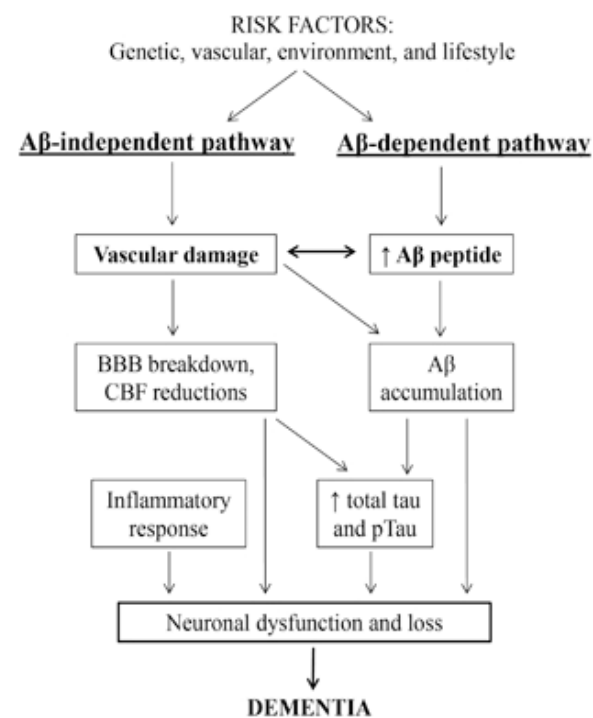


Figure 1. Multifactorial model of developing dementia or AD. Illustrating two pathways, the A β dependent and independent pathway, that are triggered by a variety of risk factors. These pathways interact and together cause neuronal dysfunction and neuronal loss leading to AD [37].

disease. In the case of AD, females seem to have a higher susceptibility to the disease compared to age-matched males (Azad, Al Bugami, & Loy-English, 2007; Launer et al., 1999). The higher incidence of AD in females might be explained (partly) by the higher susceptibility to AD risk factors. Females over the age of 75 have a higher prevalence of hypertension, hyperlipidemia and diabetes compared to age-matched men. These are all factors that are associated with the development of AD (Azad et al., 2007). In APP mice, females have a higher level of A β 40 and A β 42 in the hippocampus at four months of age. Female mice also have a higher plaque number and heavier A β burden at both 12 and 17 months of age (Wang, Tanila, Puoliväli, Kadish, & van Groen, 2003).

Compared to age-matched females males have a higher incidence rate for stroke, but women have an overall higher prevalence rate and more severe strokes (Kim, Lee, Roh, Ahn, & Hwang, 2010). Age is an important risk factor for stroke (Sahathevan et al., 2012). Women live longer and are therefore more likely to suffer from stroke (Appelros, Stegmayr, & Terént, 2009). Furthermore, a division between pre and post menopause should be made. Studies have shown that premenopausal women experience fewer strokes than men, but postmenopausal women experience more strokes than age-matched men. Estrogen has proven to protect against AD (Haast, Gustafson, & Kiliaan, 2012). After menopause, estrogen levels will drop and the chance of developing AD increases. This postmenopausal phenomenon, and the fact that the women on average live longer, lead to the fact that the onset of the stroke and therefore the severity and mortality of the stroke is higher in women (Haast et al., 2012). Furthermore, men seem to be more prone to ischemic stroke than women, while women are more prone to subarachnoid hemorrhage, regardless of age (Appelros et al., 2009). Unfortunately, only few studies on AD, vascular factors, and the interaction use both male and female models. A lot is still unclear about the consequences of sex on either AD, stroke, or the combination of both.

Although a lot of research has been done on the development of AD (de la Torre, 2004), there is much still unclear about the sex differences and the interaction of AD and stroke. Animal research plays an important role in better understanding the interaction between AD, stroke, and gender. One animal model that is widely used to study AD is the APP^{swe}/PS1^{dE9} (APP) mouse model (Jankowsky et al., 2001). These mice contain human transgenes for both APP and PSEN1 (Goodwin et al., 2019),

which are not naturally expressed in mice. Both A β 42 and A β 40 levels increase with age, but A β 42 levels are especially elevated in these mice (Jankowsky et al., 2003). Amyloid deposits appear first in the cortex at 6 weeks of age, in the hippocampus at 3 months of age and finally in the striatum, thalamus and brain stem at around 4 or 5 months of age. The specific A β burden differs per sex. Female mice reach the maximum level of deposits around 9 months of age, while male mice reach this maximum at around 12 months of age (Ordóñez-Gutiérrez, Antón, & Wandosell, 2015). Dendritic spine loss appears around the plaques approximately 4 weeks after plaque formation and eventually at 7 months of age, mice start showing cognitive impairments. A gradual reduction in GLUT-1 between 8 and 18 months of age has been reported in this model too (Hooijmans et al., 2007).

Current study

This study focused on the long-term relationship between AD and vascular risk factors, both in male and female mice. The current study will investigate the effects of stroke, AD and gender on synaptic density and A β plaques in the mouse brain, both markers for AD pathology. The precise relation between stroke and AD is still unclear. Studies on this topic are limited and often not of a longitudinal nature (Kemppainen, Hämäläinen, Miettinen, Koistinaho, & Tanila, 2014).

To do this, a mouse model of AD, expressing A β , was subjected to a transient middle cerebral artery occlusion in the right hemisphere of the brain to mimic a stroke. Since the left hemisphere did not suffer from any reduced blood flow, a within-subject control (left compared to right hemisphere) can be used next to the overall control group. Animals were sacrificed 8 months after stroke induction to investigate the long-term effects of AD and stroke.

Via quantitative polymerase chain reaction (qPCR), synaptophysin was analyzed as an indicator for synaptic density, and A β was analyzed via enzyme-linked immune sorbent assay (ELISA) and immunohistochemical stainings (IHC). Multiple areas will be analyzed via A β staining.

It is important to investigate the effect of stroke and AD in both males and females, since sex differences play an important role in both AD and stroke. It is expected that the stroke will have an aggravating effect on the AD mouse model, shown by increased A β deposits.

Synaptic density could be decreased in APP animals as a result of AD pathology. It is expected

that the synaptic density is further decreased by stroke induction, which will present as a further decrease in synaptic density in the combined AD-stroke mice. When comparing male and female mice, it is expected that the female mice will have a stronger reaction to the stroke, represented by decreased synaptic density, since females seem to recover less than age matched controls over time (Kim et al., 2010). Furthermore, female APP mice are expected to have a heavier A β burden compared to male APP mice, as shown before in other studies (Wang et al., 2003).

Methods

Animals

This study involved the use of two strains of mice: the APP^{swe}/PS1^{dE9} (APP) mice as a model for AD and the C57B1/6 wildtype (WT) littermates. For both strains, male and female mice were included. The APP^{swe}/PS1^{dE9} founder mice were obtained from John Hopkins University, Baltimore, MD, USA (Jankowsky et al., 2003). A colony was bred at the Central Animal facility at the Radboud University medical center in the Netherlands. Originally, the line was maintained on a hybrid background by backcrossing to C3HeJxC57BL/6J F1 mice. For this study, the desired mice were created by backcrossing the breeder mice to C57BL/6J for fifteen generations. At 3 months of age, the APP mice start to express amyloid beta plaques in their brain (Radde et al., 2006).

Mice were housed at 21°C, at an artificial 12:12h light-dark cycle (lights on at 7 a.m.) and were housed with a maximum of six animals per cage. After surgery, mice were housed individually in digital ventilated cages (DVC) for 24/7 activity monitoring

(Tecniplast, Buggiate, Italy).

Water and food (Sniff rm/h V1534, Bio Service, Uden, The Netherlands) were available *ad libitum*. Experiments were performed according to Dutch federal regulations for animal protection and were approved by the Veterinary Authority of Radboud University medical center in Nijmegen, the Netherlands, and the Animal Experiment Committee of the Radboud University in Nijmegen, the Netherlands (dierenexperimentencommissie, DEC, 2012-248 & 2015-0079).

Study design

Animals were divided in eight groups, depending on genotype, surgery, and sex (Table 1). A total of 144 mice were included in the study. Ninety-two mice completed all experiments. An estimation of 14 animals per group was made to reach sufficient power. All animals were randomly divided between stroke and sham, considering an equal division of sex.

During postmortem procedures and all data analyses, researchers remained double blinded for experimental groups.

Due to the large number of animals, and the longitudinal aspect of this study, the experiment was divided in multiple cohorts, each containing the same experimental structure and design. Animals from each experimental group were distributed evenly over the different cohorts. The cohorts were distributed over 2 years (cohort 1&2: May 2016-May 2017, cohort 3&4: February 2017-April 2018, cohort 5&6: September 2017-August 2018).

Different tests were performed before and after stroke induction, to assess health and behavior of the mice (Fig. 2). At three and a half months of age general health parameters body weight and systolic

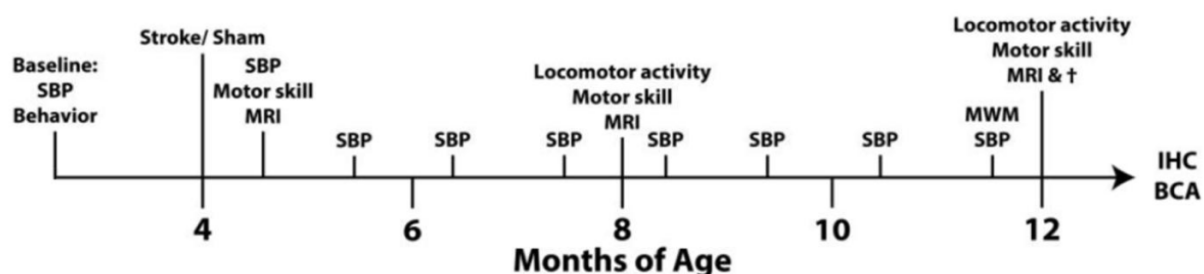


Figure 2. Overview of the current study design. A timeline of the study. Baseline SBP and behavior were assessed at 2.5 months. Stroke was induced at four months of age. At 4.5, 8 and 12 months, behavior, cognition, motor skill and locomotor activity were assessed by performing the pole test, grip test and open field. At the same timepoints, MRI was performed. At 12 months of age, rotarod and MWM were performed. After the last tests at 12 months of age animals were sacrificed, and their brains were obtained for IHC and BCA. SBP: systolic blood pressure. MWM: Morris water maze. IHC: immunohistochemistry. BCA: biochemical analysis.

Table 1. Animal groups. An overview of the animal groups with all differential characteristics, including group size (n). APP = APP^{swe}/PS1^{dE9} mice model for AD. WT = wildtype.

Strain	APP				WT			
	Stroke		Sham		Stroke		Sham	
Sex	♂	♀	♂	♀	♂	♀	♂	♀
n	8	9	9	9	12	14	14	15
Group name	1: APP - Stroke - Male	2: APP - Stroke - Female	3: APP - Sham - Male	4: APP - Sham - Female	5: WT - Stroke - Male	6: WT - Stroke - Female	7: WT - Sham - Male	8: WT - Sham - Female

blood pressure (SPB) were measured. Baseline behavior and motor skills were assessed for all mice via the pole test, grip test and open field test.

At four months of age either the stroke or sham operation was performed. Two weeks after the operation all behavioral tests were repeated and imaging was conducted (resting state functional magnetic resonance imaging (rsfMRI), diffusion tensor imaging (DTI) and flow-sensitive alternating inversion recovery-arterial spin labeling (FAIR-ASL), to assess the effects of the surgery. SBP measurements were repeated every month. Imaging, motor skill, and behavioral assessments were repeated at eight and 12 months of age. At 12 months of age, the rotarod test and the Morris water maze were performed in addition to the other tests. All behavioral procedures were performed during daytime. Afterwards, all animals were sacrificed via transcardinal perfusion and tissues were collected for postmortem analyses.

Postmortem analysis was done after tissues of all cohorts were collected. The order of all postmortem analyses was randomized for cohort numbers.

Transient occlusion of the middle cerebral artery

At four months of age, ischemic stroke was induced via a 30 minute transient occlusion of the middle cerebral artery (MCAO) in the right hemisphere (Fig. 3, (Bertrand, Dygert, & Toborek, 2017)). 5 mg/kg Rimadyl was injected before surgery, to prevent inflammation and pain during recovery. Animals were anesthetized with 2-3% isoflurane (Abbott Animal Health, Abbott park USA) and maintained on 1,5% isoflurane during the surgery. The monofilament (Doccol corporation, Sharon USA, 7-0 monofilament, 190-200 µm diameter, 2-3 mm coating) was inserted via the common carotid artery (CCA), through the internal carotid artery (ICA) up to the middle cerebral artery (MCA). Cerebral blood flow was monitored with a Laser doppler flow probe (moorVMS-LDF2, Moor

Instruments). Occlusion was maintained for 30 minutes and the surgery was deemed successful if an 80% drop in regional cerebral blood flow was reached. For the control group the filament was introduced shortly, but was retracted immediately after reaching the MCA. During the first week after surgery mice were checked daily for signs of discomfort or stress.

Biochemistry

At 12 months of age, the mice were sacrificed via transcardinal perfusion using 0.1M phosphate-buffered saline (PBS) followed by a solution of 4% paraformaldehyde in 0.1M PBS. Tissues from the ears, eyes, brain, heart, aorta, and CCA were collected, as well as some cerebral spinal fluid (CSF). The brains were cut in a transversal plane, such that part of the stroke was present in both the frontal and ventral part. The frontal brain half was divided in the left and right hemisphere and used to isolate deoxyribonucleic acid (DNA), ribonucleic acid (RNA), and proteins.

RNA was collected and prepared for qPCR (Supplementary protocol 1-4). Next to the RNA concentrations Nanodrop measures also provides measurements which can be used as quality control and purity check. There were some samples that were outside of the advised range. These samples were checked for abnormalities regarding the qPCR results, both for primary outcomes and melting curves. For the cDNA synthesis, 400 ng of total RNA was used. QPCR was performed using SYBRGreen as a reagent, for glucose transporter 1 (GLUT-1), synaptophysin (SYP) and housekeeping gene beta-2 microglobin (B2M) (Supplementary protocol 5). Supplementary protocol 2 to 4 were redone for samples which had abnormal values for the housekeeping gene B2M. Thresholds for the Ct values were set at 0.08.

DNA was collected either via an ear clip or via postmortem isolation of the brain tissue (Supplementary protocol 6). Genotyping was

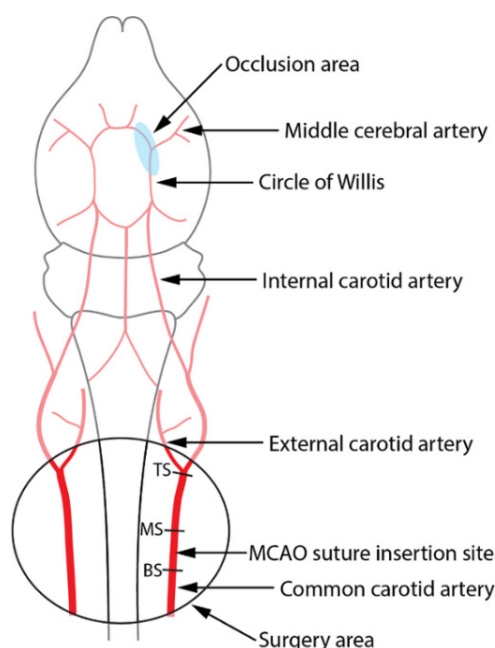


Figure 3. Induction of ischemic stroke. The incision was made in the neck of the animal (surgery area). The filament was inserted in the right common carotid artery and pushed up to the middle cerebral artery (the occlusion area). The filament was held in place for 30 minutes.

performed on an agarose gel (Supplementary protocol 7).

The protocol for protein isolation was derived from Simões et al. (2013) and adjusted to fit this study (Supplementary protocol 7). Proteins were only isolated from APP mice, since the WT mice do not express the proteins of interest, amyloid beta. Protein concentrations were adjusted to each hold 25 ng in 50 μ L. ELISA was performed for the amyloid beta 40 and 42 proteins, using the protocols Human A β 42 ELISA kit (KHB3441, invitrogen) and Human A β 40 ELISA Kit (KHB3481, invitrogen). Concentrations were determined via calibration samples and calculated to the unit of pg/ng.

Immunohistochemistry

The posterior brain halves were postfixed in 4% paraformaldehyde overnight at 4°C. The next day, brains were separately transferred to a solution containing 0.1M PBS and 0.01% sodium azide. Brains were cryoprotected in 30% sucrose in phosphate buffer for 24h before cutting. This part of the brains was used for immunostaining of GLUT-1 and A β . Brains were cut in eight series of 30- μ m-thick coronal sections using a freezing sliding microtome (Microm HM 450, Walldorf, Germany). Brain sections were stored in 0.1M PBS with 0,01% sodium azide at 4°C before immunohistochemical

staining. In total two immunohistochemical stainings were performed using standard free-floating labelling procedure at room temperature. For each staining, one subseries of brain sections per animal was used. After every incubation step, brain sections were rinsed 3 times for 15 minutes in 0.1M PBS for the GLUT-1 staining. For the A β staining, brain sections were rinsed in tris Buffered Saline + 0,5% Triton (TBS-T).

All free-floating brain sections were rinsed with 0.1M PBS for 15 minutes and treated with 0.3% H₂O₂ in 0.1M PBS for 30 minutes. Next, brain sections were pre-incubated in 2 ml 0.1M PBS-BT for 30 minutes. For A β staining, the brain sections were pre-incubated in 2 ml 0.05M Tri-sodium citrate solution at 85°C for 30 minutes. After this pre-incubation step, primary anti-bodies (GLUT-1: rabbit anti-GLUT-1 [1:40.000; Millipore, Billerica, MA, USA] or WO-2: mouse anti-human A β 4-10 [1:10.000; Centre for Molecular Biology, University of Heidelberg, Germany]) were added overnight. After rinsing, secondary anti-bodies (GLUT-1: donkey anti-rabbit [1:1500; Jackson ImmunoResearch, West Grove, PA, USA], WO-2: donkey anti-mouse biotin [1:1500; Jackson ImmunoResearch, West Grove, PA, USA]) were added for 1.5 h followed by incubation with ABC-Elite (1:800; GLUT-1 in PBS-BT, A β in TBS-T) for 1.5h. Afterwards, all brain sections were pre-incubated in DAB-Ni for 10 minutes followed by incubation in DAB-Ni with 30% H₂O₂ for 10 minutes. Brain sections were mounted on gelatine-coated slides (0.5% gelatine and 0.05% chrome-alum) and dried at 37°C overnight. The slides were dehydrated with alcohol, cleared with xylol and coverslipped with Entellan.

Quantification

The stained sections were viewed with a 5x objective Axio Imager A2 (Zeiss Germany), and ZEN software was used for image acquisition. Brain sections were preselected according to the mouse brain atlas of Franklin and Paxinos [66]. The regions of interest (ROIs) for A β contain the cortex, hippocampus and thalamus (bregma: -1.94), as reference areas which do not directly get blood supply from the MCA, and the cortex, corpus callosum and basal ganglia (bregma: 0.62), areas which are partially or directly supplied by the MCA. The analysis of all images was performed using ImageJ (National Institute of Health, Bethesda, MD, USA). For the A β staining the average plaque size, relative positive A β area, and number of plaques per area (mm²) were calculated.

Data analysis

All statistical analyses were preformed using IBM SPSS 25 software (IBM Corporation, New York, NY, USA). Data were split on genotype, surgery, and sex and checked for outliers. Two animals were excluded for the analyses of the ELISA for A β 40 and A β 42, because of extremely deviant values.

Differences between sex (male/female), surgery (sham/stroke), and hemispheres (left/right) were determined. Repeated measures ANOVA with Bonferroni corrections were used to determine significant differences between the left and right hemispheres. Multivariate ANOVA with Bonferroni corrections to determine significant differences between surgery and/or sex. Data were checked for interaction between the variables, and further split if necessary. GraphPad Prism (6.01, GraphPad Software, La Jolla California, USA) was used to create all presented figures. All data are presented as mean \pm SEM. Data were considered significant if $p \leq 0.05$.

$0.08 \geq p \geq 0.05$, * $p \leq 0.05$, ** $p \leq 0.01$, *** $p \leq 0.001$.

Results

An overview of the various results can be found in Supplementary table 1.

Genotype

All animals were genotyped at the start and the end of the experiment. The PrP gene is present in all mice, while the hAPP gene is only present in the APP mice. WT mice only show one band at 750 bp, while the APP mice show two bands, at 750 bp and 400 bp. No abnormalities were seen regarding genotype and all expression patterns were complementary to the 'assumed' genotype (APP vs WT) of the individual animals (Fig. 4).

Amyloid beta burden in the frontal brain

To determine the level of A β , proteins were isolated from the frontal part of the brain, including parts of the ischemic core and the penumbra. Proteins were isolated from the brains of all APP mice. ELISA for A β 40 and A β 42 were performed and the ratio between the two A β proteins was determined. No significant differences between the left and right hemisphere were found regarding A β 40, A β 42 or the A β 42/A β 40 ratio (Fig. 5).

Female APP mice showed a higher concentration of A β 40 in both the left ($p < 0.006$) and right ($p < 0.024$) hemisphere compared to male APP mice (Figure 6A). No significant differences between females and males were found regarding A β 42 or the A β 42/A β 40 ratio (Figure 6B-C). No significant difference between stroke APP and sham APP mice were found regarding A β 40, A β 42 or the ratio A β 42/A β 40 (Figure 6A-C).

Amyloid beta burden in ischemic and unaffected regions

To further determine the level of A β brain sections of APP mice were immunohistochemically stained for A β at bregma 0.62, close to the ischemic core and at bregma -1.94 further away from the ischemic region. At bregma -1.94 the cortex (Fig. 7A), hippocampus (Fig. 7B), and thalamus (Fig. 7C) were analyzed for differences in the average plaque size, relative A β positive area, and the number of A β plaques per area (mm^2). A trend was visible in the cortex in male sham ($p < .067$) and female stroke ($p < .075$) mice, in which the right hemisphere seems to have a higher average plaque size compared to the left hemisphere. No significant differences were found between the left and right hemisphere in the cortex regarding relative A β area or number of A β plaques per area (mm^2). No significant differences were found between the left and right hemisphere in the hippocampus regarding average plaque size. Female stroke mice showed a significant increase ($p < .032$) in relative A β area in the right hemisphere compared to the left hemisphere in the hippocampus. A trend ($p < .07$) was visible in the female stroke mice, in which the right hemisphere tended to have an increased number of A β plaques per area (mm^2) compared to the left hemisphere in the hippocampus. Female sham mice showed a significant increase in average plaque size in the right hemisphere compared to the left hemisphere ($p < .003$). No significant differences were found between the left and right hemisphere in the thalamus in relative A β area or number of A β plaques per area (mm^2).

Brain sections of APP mice were also immunohistochemically stained for A β at bregma 0.62, close to the ischemic core. At bregma 0.62, the cortex (Fig. 8A), corpus callosum (Fig. 8B) and basal ganglia (Fig. 8C) were analyzed for differences in the average plaque size, relative A β positive area and the number of A β plaques per area (mm^2). Male stroke mice showed a significant decrease in average plaque size ($p < .03$), relative A β area ($p < .004$) and number

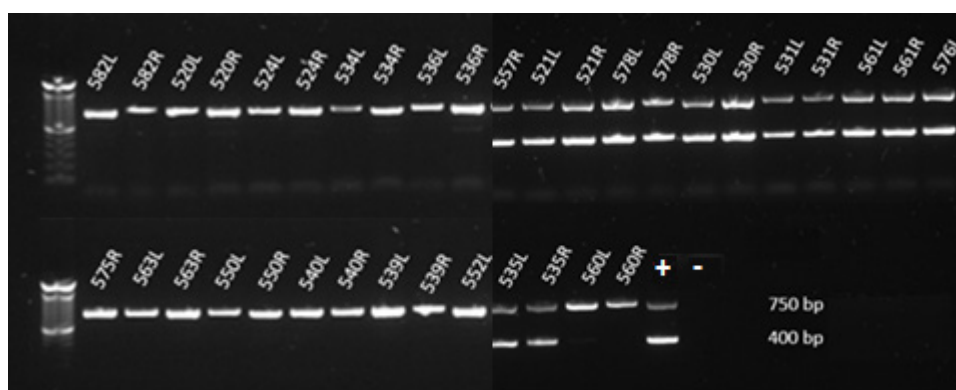


Figure 4. Genotyping by agarose gel. Representative photo of samples of the genotyping performed on an agarose gel. Other gels were performed in a similar way. WT animals only show one band at 750 bp (top band, PrP gene), the APP mice have two bands, at 750 bp (top band, PrP gene) and 400 bp (lower band, APP gene). Numbers refer to the animal number. L: left hemisphere, R: right hemisphere, +: positive control, -: negative control.

of A β plaques per area (mm²) ($p < .038$) in the right hemisphere compared to the left hemisphere in the cortex. No significant differences were found between the left and right hemispheres in the corpus callosum regarding average plaque size or relative A β area. Male sham animals showed a significant increase in number of A β plaques per area (mm²) in the right hemisphere compared to the left hemisphere ($p < .032$) in the corpus callosum. No significant differences were found between the left and right

hemispheres in the basal ganglia regarding average plaque size. Female stroke mice showed a significant decrease ($p < .042$) in relative A β area in the right hemisphere compared to the left hemisphere in the basal ganglia. No significant differences were found between the left and right hemispheres in the basal ganglia in number of A β plaques per area (mm²).

Data from bregma -1.94, the cortex (Fig. 9A), hippocampus (Fig. 9B), and thalamus (Fig. 9C) were further compared for sex (male vs female) and

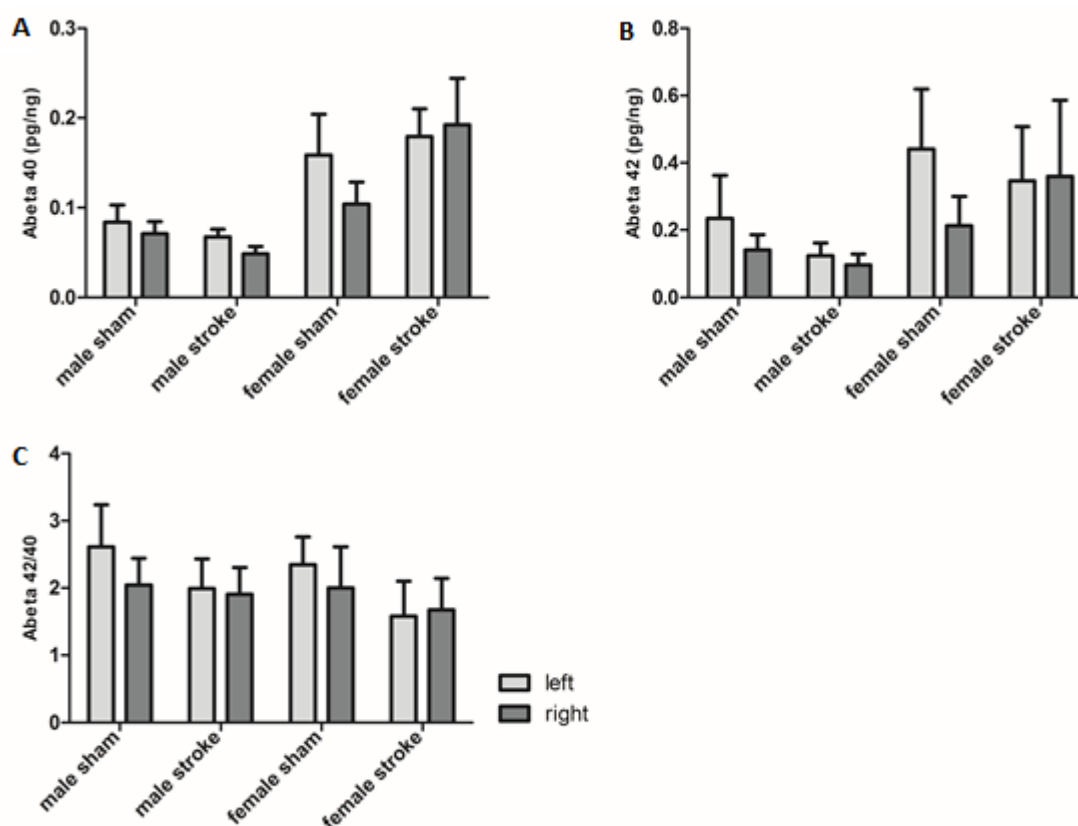


Figure 5. Concentration of Amyloid beta in the frontal part of the brain, L vs R effects. All data are presented as mean \pm SEM. No significant differences between the left and right hemisphere were found regarding the concentration of A β 40 (A), A β 42 (B) or the ratio of A β 42/A β 40 (C).

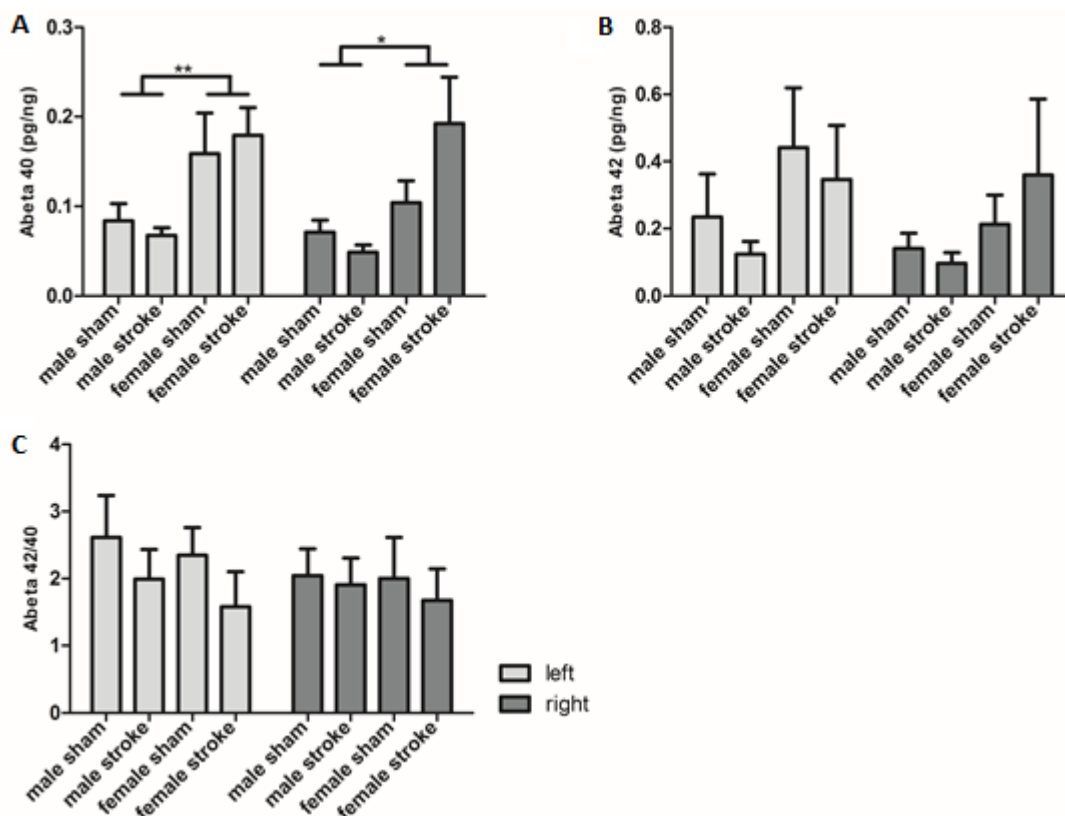


Figure 6. Concentration of Amyloid beta in the frontal part of the brain, sex, and surgery effects. All data are presented as mean \pm SEM. The concentration of A β 40 was increased in female mice compared to male mice in both the left ($p < .006$) and the right ($p < .024$) hemisphere (A). No significant sex or surgery differences were found regarding the concentration of A β 42 (B) or the ratio of A β 42/A β 40 (C).

surgery (sham vs stroke) differences. No significant differences were found in the cortex between males and females regarding average plaque size, relative A β area, or number of A β plaques per area (mm^2). No significant differences were found in the hippocampus between males and females regarding average plaque size. Female mice showed a significant increase in relative A β area in both left ($p < .044$) and right ($p < .012$) hemisphere compared to males in the hippocampus. Female mice also displayed a significant increase in number of A β plaques per area (mm^2) in both left ($p < .025$) and right ($p < .019$) hemisphere compared to males in the hippocampus. A significant increase in average plaque size ($p < .042$) in the right hemisphere and in relative A β area in both left ($p < .012$) and right ($p < .003$) hemisphere was found in female mice compared to male mice in the thalamus. And furthermore, a significant increase in number of A β plaques per area (mm^2) ($p < .030$) in the left hemisphere of the thalamus was seen in female mice compared to male mice. No significant differences between stroke and sham APP mice were found regarding relative A β area or number of A β plaques per area (mm^2). No interactions were found between sex and surgery.

Differences in sex and surgery were also

analysed in the cortex (Fig. 10A), hippocampus (Fig. 10B) and thalamus (Fig. 10C) on bregma 0.62. No significant differences were found in the cortex between males and females regarding average plaque size. In the cortex, the relative A β area in the right hemisphere ($p < .003$) and in number of A β plaques per area (mm^2) in both the left ($p < .031$) and right ($p < .001$) hemisphere was significantly increased in female mice compared to male mice. No significant differences were found in the corpus callosum between males and females regarding average plaque size, relative A β area, or number of A β plaques per area (mm^2). Female mice presented with a significant increase in the basal ganglia in average plaque size ($p < .033$) in the right hemisphere. A trend was visible in the basal ganglia in the right hemisphere, in which stroke mice seem to have a lower average plaque size compared to sham mice ($p < .073$). A significant increase in relative A β area in the left hemisphere ($p < .004$) was found in female mice compared to male mice. A trend ($p < .069$) was visible in the right hemisphere where female mice seem to have an increased number of A β plaques per area (mm^2) compared to the left hemisphere. Female mice showed a significant increase in number of A β plaques per area (mm^2) in both the left ($p < .001$) and

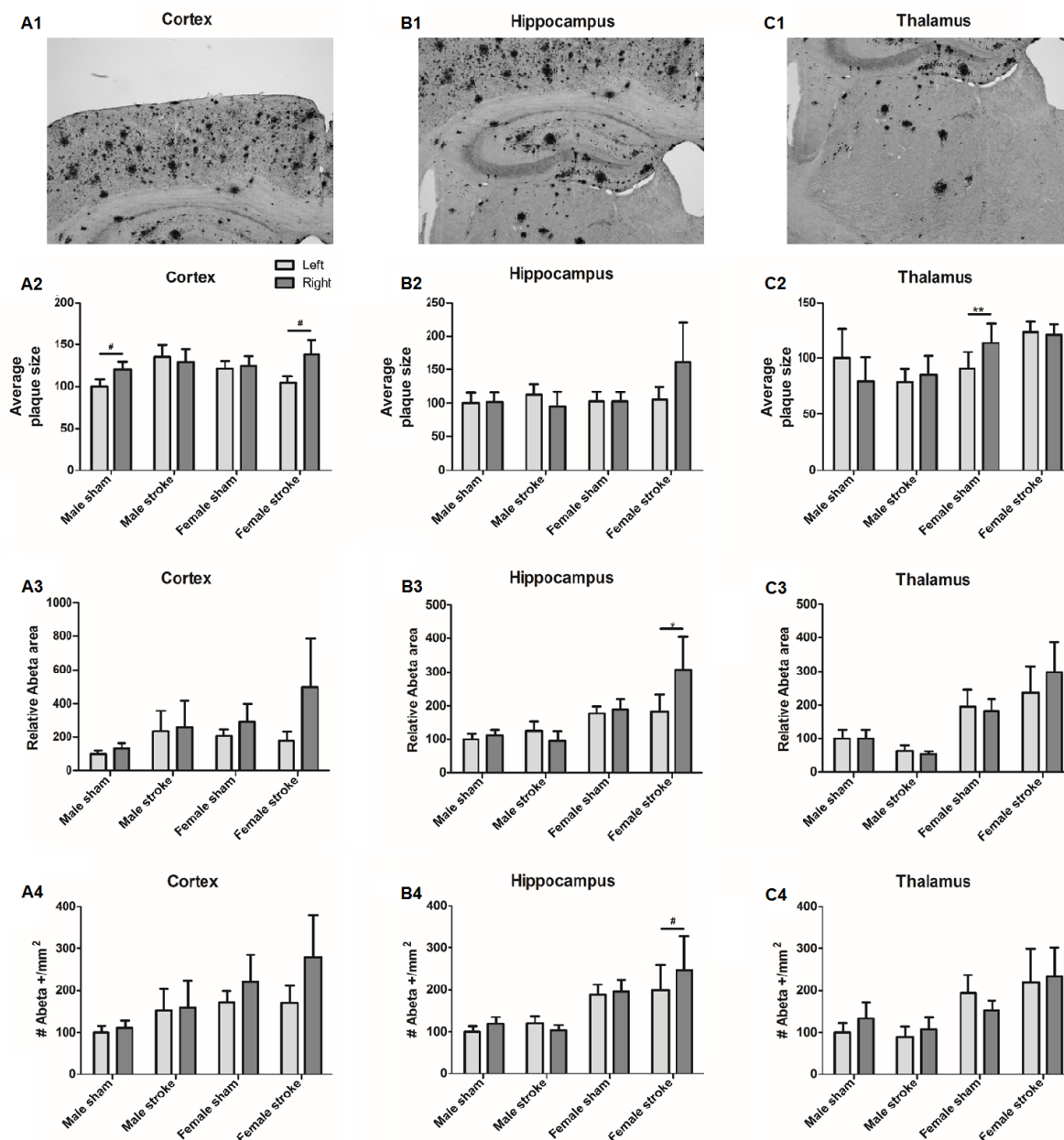


Figure 7. Average plaque size, relative A β positive area and number of A β plaques per area (mm²) in the cortex, hippocampus, and thalamus (bregma -1.94) of APP mice, L vs R effects. All data were normalized against the left male sham group and presented as mean \pm SEM. A representative photo of the A β staining of the right hemisphere of the cortex is shown (A1). A trend was visible in the average plaque size in the cortex in which the right hemisphere has a higher average plaque size than the left hemisphere in both male sham ($p < .067$) and female stroke animals ($p < .075$) (A2). No significant differences between the left and right hemispheres were found in the cortex regarding relative A β positive area (A3) or number of A β plaques per area (mm²) (A4). A representative photo of the A β staining of the right hemisphere of the hippocampus is shown (B1). No significant differences between the left and right hemispheres were found in the hippocampus regarding average plaque size (B2). Relative A β positive area was increased in the hippocampus in the right hemisphere compared to the left hemisphere ($p < .032$) in female stroke mice (B3). A trend was visible in number of A β plaques per area (mm²) ($p < .070$) in the hippocampus, in which the right hemisphere has a higher amount of A β plaques than the left hemisphere (B4). A representative photo of the A β staining of the right hemisphere of the thalamus is shown (C1). Average plaque size was increased in the thalamus in the right hemisphere compared to the left hemisphere ($p < .003$) in female sham mice (C2). No significant differences between the left and right hemisphere were found in the thalamus regarding relative A β positive area (C3) or number of A β plaques per area (mm²) (C4).

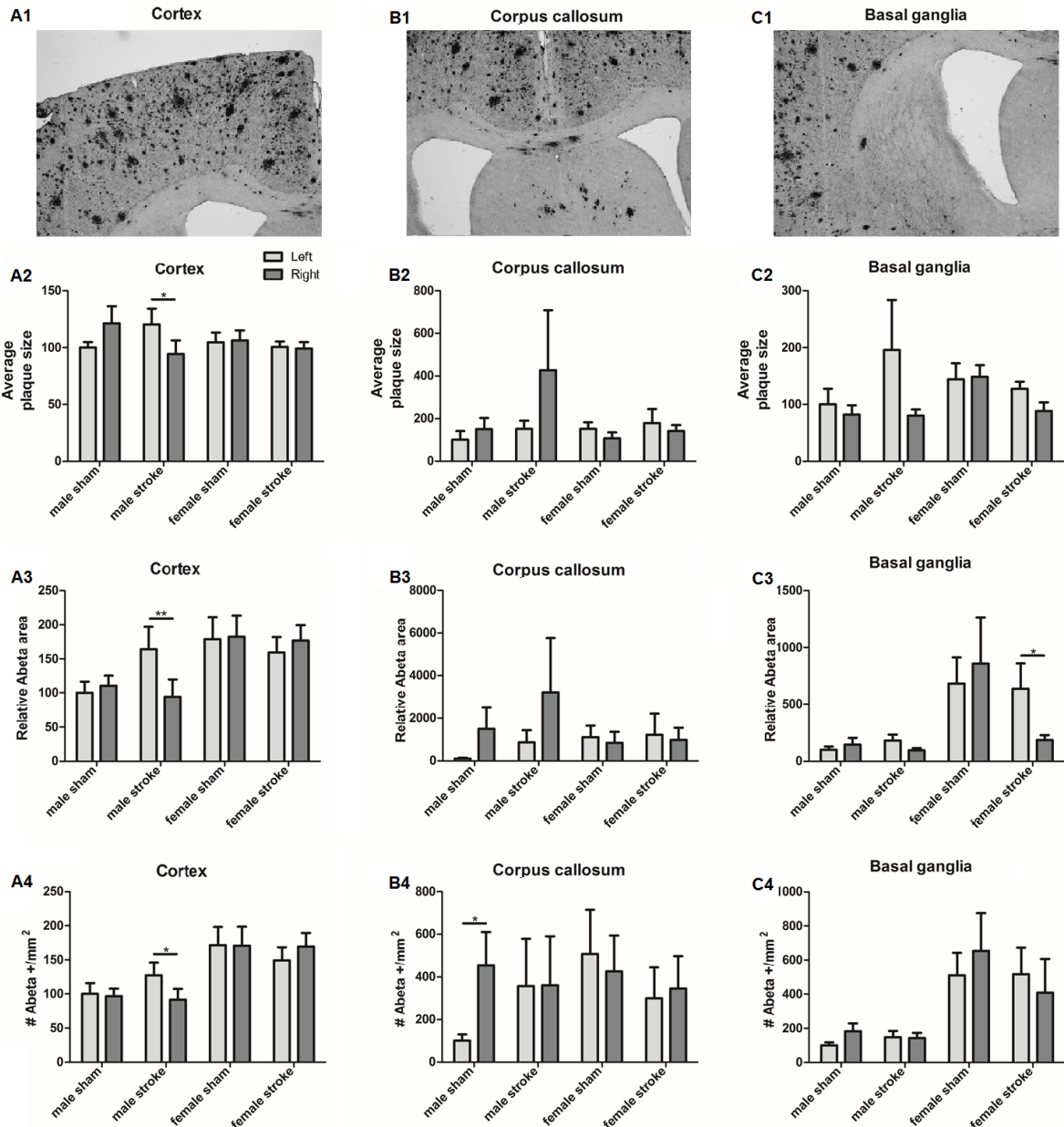


Figure 8. Average plaque size, relative A β positive area and number of A β plaques per area (mm²) in the cortex, corpus callosum, and basal ganglia (bregma 0.62) of APP mice, L vs R effects. All data were normalized against the left male sham group and presented as mean \pm SEM. A representative photo of the A β staining of the right hemisphere of the cortex is shown (A1). Average plaque size was decreased in the cortex in the right hemisphere compared to the left hemisphere ($p < .030$) in male stroke mice (A2). Relative A β positive area was decreased in the right hemisphere compared to the left hemisphere ($p < .004$) in male stroke mice (A3). Number of A β plaques per area (mm²) was decreased in the cortex in the right hemisphere compared to the left hemisphere ($p < .038$) in male stroke mice (A4). A representative photo of the A β staining of the right hemisphere of the corpus callosum is shown (B1). No significant differences between the left and right hemisphere were found in the corpus callosum regarding the average plaque size (B2) or relative A β positive area (B3). Number of A β plaques per area (mm²) was increased in the corpus callosum in the right hemisphere compared to the left hemisphere ($p < .032$) in male sham mice (B4). A representative photo of the A β staining of the right hemisphere of the basal ganglia is shown (C1). No significant differences between the left and right hemispheres were found in the basal ganglia regarding average plaque size (C2). Relative A β positive area was decreased in the basal ganglia in the right hemisphere compared to the left hemisphere ($p < .042$) in female stroke mice (C3). No significant differences between the left and right hemisphere were found in the basal ganglia regarding the number of A β plaques per area (mm²) (C4).

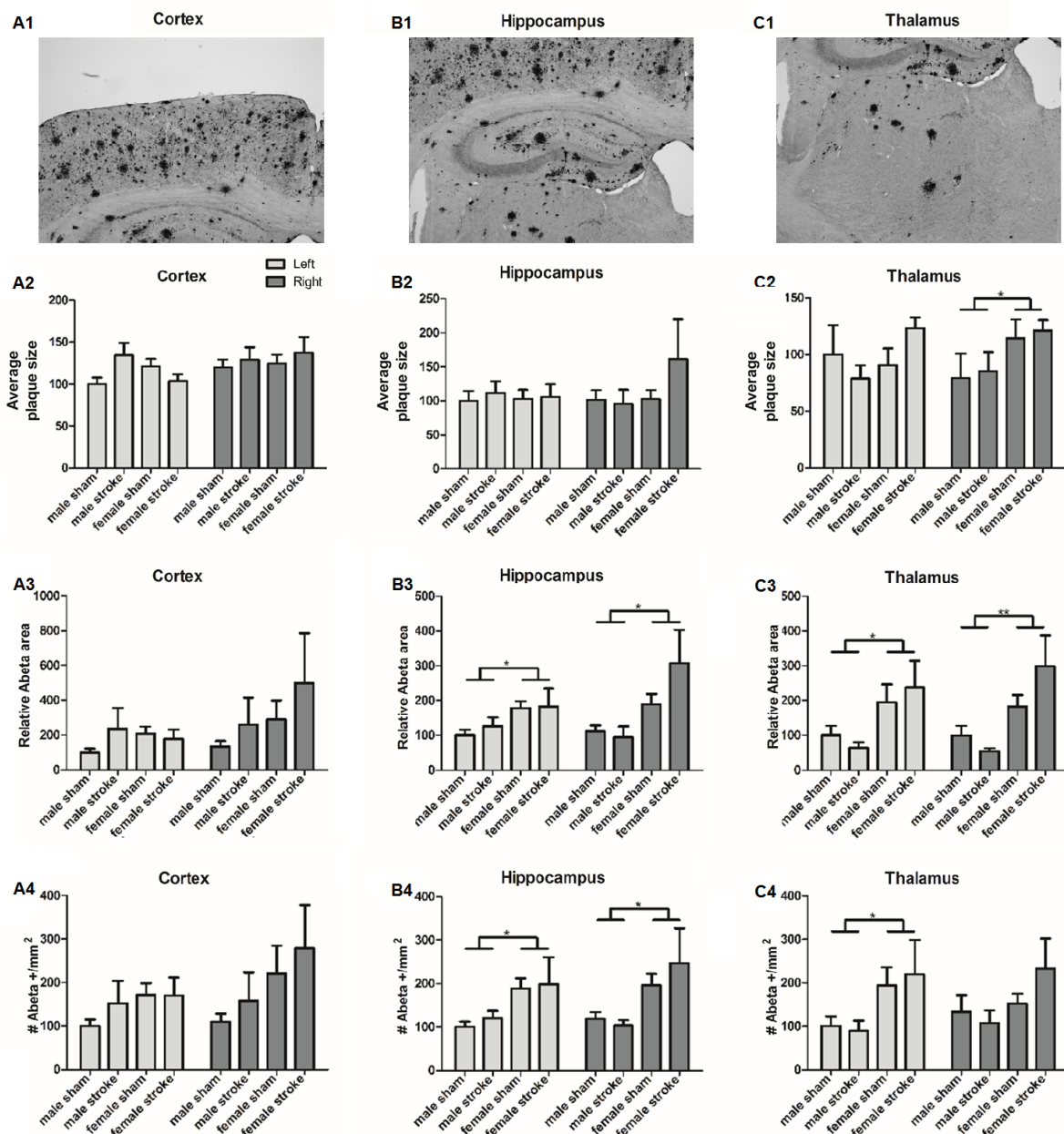


Figure 9. Average plaque size, relative A β positive area and number of A β plaques per area (mm²) in the cortex, hippocampus, and thalamus (bregma -1.94) of APP mice, sex and surgery effects. All data were normalized against the left male sham group and presented as mean \pm SEM. Representative photo of the A β staining of the right hemisphere of the cortex is shown (A1). No significant differences between sex or surgery were found in the cortex regarding average plaque size (A2), relative A β positive area (A3) or number of A β plaques per area (mm²) (A4). A representative photo of the A β staining of the right hemisphere of the hippocampus is shown (B1). No significant differences between sex or surgery were found in the hippocampus regarding average plaque size (B2). Relative A β positive area was increased in the hippocampus in female mice compared to male mice in both the left ($p < .044$) and right ($p < .012$) hemisphere (B3). Number of A β plaques per area (mm²) was increased in the hippocampus in female mice compared to male mice in both left ($p < .025$) and right ($p < .019$) hemisphere (B4). A representative photo of the A β staining of the right hemisphere of the thalamus is shown (C1). Average plaque size was increased in the thalamus in female mice compared to male mice ($p < .042$) in the right hemisphere (C2). Relative A β positive area was increased in the thalamus in female mice compared to male mice in both the left ($p < .012$) and right ($p < .003$) hemisphere (C3). Number of A β plaques per area (mm²) was increased in the thalamus in female mice compared to male mice in the left hemisphere ($p < .03$) (C4). No significant differences were found between surgery in any of the regions nor parameters.

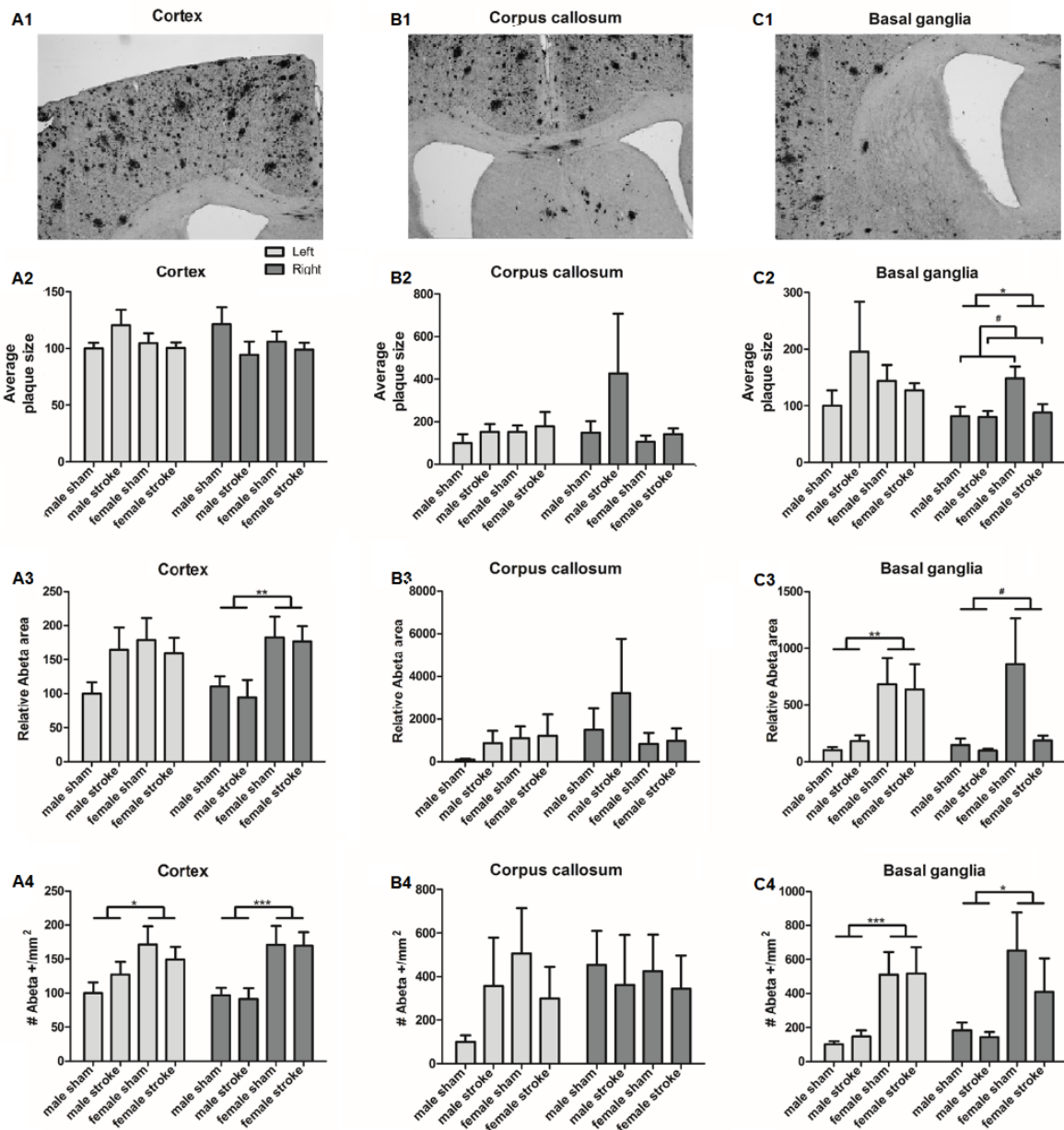


Figure 10. Average plaque size relative A β positive area and number of A β plaques per area (mm²) in the cortex, corpus callosum and basal ganglia (bregma 0.62) of APP mice, sex and surgery effects. All data were normalized against the left male sham group and presented as mean \pm SEM. A representative photo of the A β staining of the right hemisphere of the cortex is shown (A1). No significant differences between sex or surgery were found in the cortex regarding average plaque size (A2). Relative A β positive area was increased in the cortex in female mice compared to male mice in the right ($p < .003$) hemisphere (A3). Number of A β plaques per area (mm²) was increased in the cortex in female mice compared to male mice in both left ($p < .031$) and right ($p < .001$) hemisphere (A4). A representative photo of the A β staining of the right hemisphere of the corpus callosum is shown (B1). No significant differences between sex or surgery were found in the corpus callosum regarding average plaque size (B2), relative A β positive area (B3) or number of A β plaques per area (mm²) (B4). A representative photo of the A β staining of the right hemisphere of the basal ganglia is shown (C1). Average plaque size was increased in the basal ganglia in female mice compared to male mice ($p < .033$) in the right hemisphere (C2). Also, a trend was visible in the average plaque size in the basal ganglia, in which stroke animals have lower average plaque size in the right hemisphere than sham animals ($p < .073$). Relative A β positive area was increased in the basal ganglia in female mice compared to male mice in the left hemisphere ($p < .004$) (C3). A trend was visible in the relative A β positive area ($p < .069$), in which the female mice showed a higher relative A β positive area in the right hemisphere than male mice. Number of A β plaques per area (mm²) was increased in the basal ganglia in female mice compared to male mice in both the left ($p < .001$) and right ($p < .024$) hemisphere (C4). No other significant differences were found between surgery in any of the regions nor parameters.

right ($p < .024$) hemisphere compared to male mice. No other significant differences between surgeries were found regarding average plaque size, relative A β area or number of A β plaques per area (mm^2). No interactions were found between sex and surgery.

Synaptic density in affected ischemic area

Male WT sham mice showed an increased in relative synaptophysin mRNA expression in the right hemisphere (Fig. 11), compared to the left hemisphere ($p < .024$). Relative synaptophysin mRNA expression was decreased in the right hemisphere compared to the left hemisphere in the female WT sham group ($p < .026$).

Data of synaptophysin mRNA expression were split according to genotype or sex (Fig. 12). A significant decrease ($p < .004$) in relative synaptophysin expression was shown in the right hemisphere in female WT sham mice compared to male WT sham mice (Fig. 12A). Furthermore, relative synaptophysin expression was decreased ($p < .024$) in female APP mice compared to male APP mice in the left hemisphere (Fig. 12B). No significant differences were found regarding genotype or surgery in either male (Fig. 12C) or female mice (Fig. 12D).

Discussion

The overall aim of this longitudinal study was to elucidate the long-term effect of vascular damage,

caused by stroke, on AD. This report focused on the A β burden and changes in synaptic density resulting from stroke and/or AD. Furthermore, the study used both male and female animals to further investigate the sex differences present in both AD and stroke. Many aspects about the effect of stroke and AD on each other remain unclear, especially regarding the long-term effects after the stroke. Therefore, it is very important to further investigate the effect of stroke and AD markers, such as the A β burden.

Sex differences A β burden

Female APP mice had a higher A β burden than male APP mice that is present in many brain areas, including the thalamus and basal ganglia. Furthermore, the protein levels of A β 40 were also elevated in the anterior part of the brain, which became apparent by the ELISA analysis. These results were largely as expected, as an increased A β burden in the hippocampus in female APP/PS1 mice has been reported in AD mice studies before (Callahan et al., 2001; Wang et al., 2003). Wang et al. (2003) reported an increase of A β protein levels and A β burden in the hippocampus of 12-month-old female APP/PS1 mice. Callahan et al. (2001) demonstrated a similar effect in both enzyme levels and senile plaques in a different APP aging mouse model in both the hippocampus and neocortex. Wang et al. (2003) demonstrated elevated protein levels of A β 40 and A β 42, but not the A β 42/A β 40 ratio, in the hippocampus. The current results

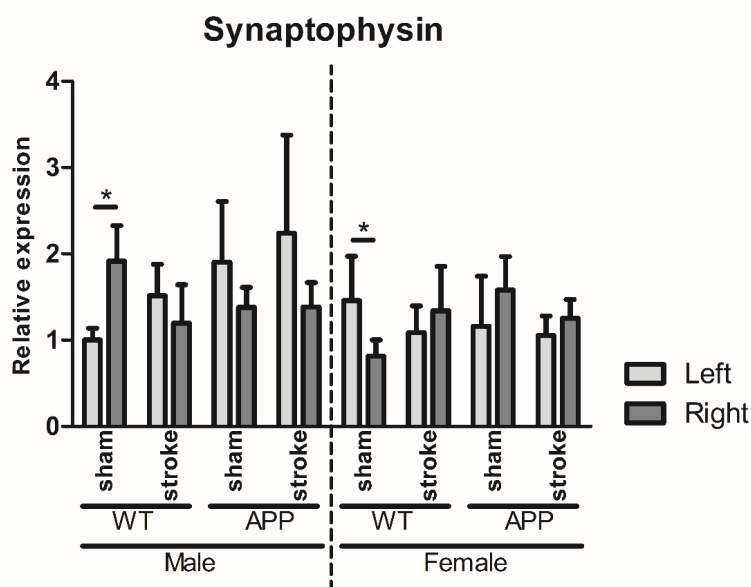


Figure 11. Relative expression of synaptophysin, L vs R effects. All data were normalized against the left male WT sham group and presented as mean \pm SEM. Relative expression of synaptophysin was increased in the right hemisphere compared to the left hemisphere in the male WT sham group ($p < .024$) and decreased right compared to left in the female WT group ($p < .026$).

showed that the gender effect in A β is not limited to the hippocampal area, and possibly the cortex, but widely spread throughout different brain areas. No significant differences in sex regarding A β 42 were found in the current study. Whether this is due to the mixture of tissues that are affected and unaffected by the stroke in this analysis or due to an insufficient power ($\alpha = 0.05$, power = 0.56) caused by high variation in the experimental group, remains unclear. But overall, such increased A β concentration and A β burden in female APP mice was found in many brain areas and is not restricted to the hippocampus and cortex.

The effects of stroke on A β burden

The A β concentration and A β burden did not significantly differ between the stroke and sham groups, suggesting that the stroke operation had

no effect on the A β burden in APP mice. Notably, there was a trend found in the right hemisphere of the basal ganglia, which indicated a decrease in the average plaque size in stroke mice compared to sham mice. This effect is most likely due to the high amount of atrophy in the area. The basal ganglia are mostly effected by the occlusion of the MCA, since they are directly supplied of oxygen and glucose by this artery (De Reuck, 1971). Supply of oxygen and glucose is severely decreased for a substantial amount of time, resulting in a high rate of cell death and atrophy in this area. The trend found in this region could therefore be associated with the atrophy and cellular apoptosis in this area.

With exception of this trend in the basal ganglia, the A β concentration and A β burden did not seem to be affected by the stroke and sham operations implying that stroke had no direct effect on the A β burden in the surrounding brain areas at bregma

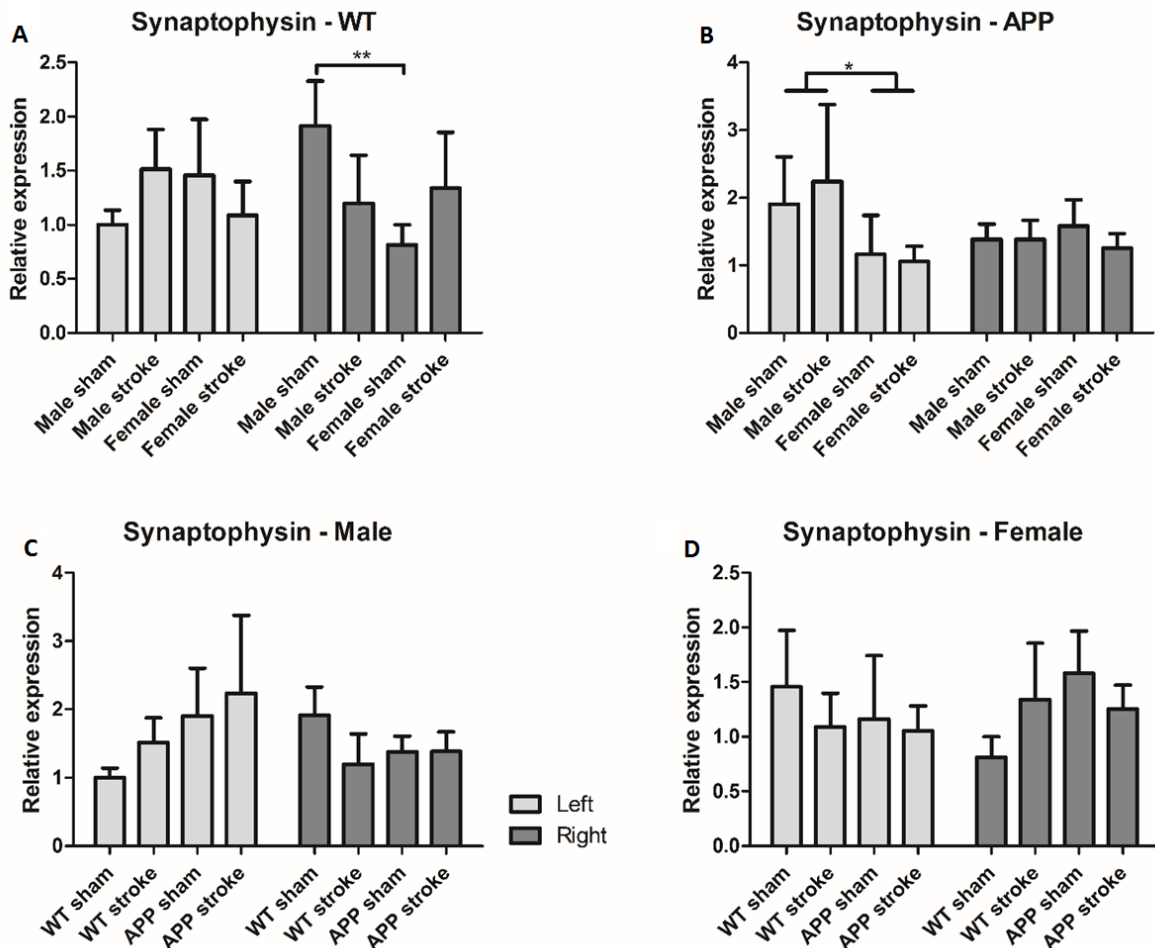


Figure 12. Relative expression of synaptophysin, sex and genotype effects. All data were normalized against the left male WT sham group and presented as mean \pm SEM. Data were split on either genotype (A-B) or gender (C-D). Relative expression of synaptophysin was decreased ($p < .004$) in the right hemisphere in female mice compared to male mice regarding the WT sham group (A). Relative expression of synaptophysin was also decreased ($p < .024$) in the left hemisphere in female APP mice compared to male APP mice (B). No significant differences were found between genotype or surgery in either male (C) or female mice (D).

of 0.62. But this conclusion cannot be drawn only from this comparison, since there were 2 controls present in this study. As mentioned before, next to the sham group serving as control, there was also a within-subject control, namely the left hemisphere of the mice. In each group only the right MCA was targeted, therefore the left hemisphere was not directly affected by the stroke operation. When the left and right hemispheres were compared with each other, stroke effects became visible. Male stroke mice showed a significant decrease in the A β burden, average size and number of plaques in the cortex of the affected hemisphere compared to the unaffected left hemisphere. This result was not expected, since studies on short-term effects reported an opposite effect of the stroke on the A β burden (Garcia-Alloza et al., 2011; Thiel, Cechetto, Heiss, Hachinski, & Whitehead, 2014) due to disruptions in amyloid clearance pathways the A β burden increased (Garcia-Alloza et al., 2011). However, mice in these studies were sacrificed days or weeks after stroke induction (Garcia-Alloza et al., 2011; Thiel et al., 2014). In the current study, mice had 8 months of recovery time. It could be that the disruption in the amyloid clearance pathway was not only minimized, but even increased due to ongoing inflammatory processes. These inflammatory processes are still present 8 months after stroke, indicated by the increased activity of reactive microglia in the male stroke animals compared to the male sham animals, that was not represented in the female animals. The expression patterns of the reactive microglia are very similar to the decrease in A β plaque patterns, indicating a correlation between the two. An interaction between microglial activity and A β plaques has been established before. However, the precise effect of microglial activity on A β clearance is very complex and can easily shift between a stimulating or inhibiting effect (Merlo, Spampinato, Caruso, & Sortino, 2020). Both positive and negative influences of microglia on A β clearance have been found, depending on the balance between pro- and anti-inflammatory activity of the microglia and the overall phenotype of the microglial cells (Merlo et al., 2020). In our case, the microglia possibly have increased the A β clearance in the affected hemisphere. This would explain why the effect was visible only in male stroke mice, since only the male mice showed an increase in microglial activity in the cortex of the affected hemisphere after stroke. To be sure about the effects of microglial activity on A β clearance a more in-depth analysis of the inflammatory response is necessary.

Areas not directly supplied by the MCA and therefore not directly affected by the stroke, showed

different patterns of A β burden. Female stroke mice showed an increase in A β burden in the hippocampus of the affected hemisphere, coupled with a trend in the number of plaques in the hippocampus and a trend in the average plaque size in the cortex (bregma -1.94).

Taken together, the A β burden was decreased in regions directly supplied by the MCA, while being increased in other brain areas. It remains unclear how stroke affects these brain regions in different manner and what role microglial activity might play in the A β clearance in this case.

Effects sham operation on A β burden

Next to the observed stroke effects, the sham groups also showed some significant differences. The female sham group showed a significant increase in average plaque size in the thalamus and there was a trend towards a higher average plaque size in the affected hemisphere of the male sham mice. A possible explanation for the observed results might be that the sham operation actually had a significant effect on the animal and the affected hemisphere. This could be possible since the filament is shortly introduced during the sham operation, blocking blood flow for a couple of seconds. Furthermore, in both sham and stroke animals after the 'occlusion', the right common carotid artery is permanently tied off and it is not clear if this effects the brain. The effect and resulting stress of the sham operation might be large enough to cause differences between the two hemispheres of the sham animals. The animals and the vascular system did undergo significant levels of stress during the surgery. Stress has been reported to contribute to the formation of A β plaques before (Han et al., 2017; Huang et al., 2015). The stress caused by the short blockage of blood flow and the overall stress of the anesthesia and operation, could possibly contribute to the formation of the A β plaques (Eckenhoff et al., 2004; Marques & Lapa, 2018) and therefore the differences between the hemispheres in the sham animals.

Along the same line, the effect of the sham operation might also explain the lack of significance between the sham and stroke animals. If the sham operation truly affects the brain in a significant manner, similar to the effect of stroke, then the lack of significance between the sham and stroke groups would be logical. It is very important to consider all factors in these sham and within-subject control models before drawing any conclusions regarding the effects or lack of effects of stroke on the A β burden. Ideally, an extra control group

without operation would have been added to further determine the effects of stress and stroke on the brain. Unfortunately, due to the already large nature of the study, this was not possible.

Furthermore, neither a sham/stroke nor a within-subject control effect was found in the results of the ELISA analyses of the anterior part of the brain. This could be caused by the chosen methodology. In the ELISA analyses, no division was made between affected and unaffected tissue because the amount of tissue was very small per animal and it was not possible to make a clear division. The effect of the stroke operation might be masked because both ischemic regions and unaffected regions are taken together for the ELISA analyses. This would weaken the differences between the different hemisphere explaining the lack of significance in this analysis compared to the IHC.

Overall, the multiple control groups and methods for analyzing A β give multiple perspectives on the research question. However, the opposing results require critical evaluation of different controls and methods used.

Asymmetric synaptic density

Next to the A β burden, this study also investigated synaptic density via determining synaptophysin mRNA expression. In this qPCR analysis an asymmetry between the two hemispheres was found in the WT sham animals. Asymmetrical expression of genes has been reported before in many animal species and in humans (Vallortigara, Chiandetti, & Sovrano, 2011). Asymmetry of synaptophysin expression specifically, has also been reported in some species, e.g. developing chicken (in both via pre and post-synaptic markers) (Roy, Nag, Upadhyay, Mathur, & Jain, 2014) and aging chimpanzees (Sherwood et al., 2010). Although asymmetry of synaptophysin has not been found before in mice, they do show some brain asymmetry and for example, paw preference (Waters & Denenberg, 1994), indicating that the mouse brain has asymmetrical properties and hemispheres are not identical. Therefore, asymmetrical expression of synaptophysin could be a possibility. However, the observed asymmetry in synaptophysin has an opposite direction in female compared to male mice: female WT sham mice showed lower synaptophysin expression in their right hemisphere compared to their left hemisphere, while male WT sham mice showed higher synaptophysin expression in their right hemisphere compared to the left one. This opposing effect in different genders has not been

reported before. Furthermore, this asymmetry is not present in any of the other experimental groups, in which the mice suffered from stroke and/or AD pathology. The sham/stroke operation and the AD pathology could influence synaptic density to such an extent that the asymmetry would be hidden. However, this would mean that the effect of stroke on synaptic density would have an opposing effect on male compared to female mice, otherwise the effect could not be concealed in both genders of the other experimental groups. To determine the true nature of this possible asymmetry, it would be beneficial to include mRNA analyses of post synaptic density marker PSD-95. A pattern of PSD-95 expression similar to the synaptophysin expression would strengthen the observed asymmetry, while a lack of similarity could suggest a false positive in the synaptophysin analyses.

Effect of AD on synaptic density

In APP mice, the effect of gender was seen in the left unaffected hemisphere. Female APP mice showed decreased expression of synaptophysin in the left hemisphere compared to male APP mice, regardless of stroke or sham operation. This effect is most likely related to the AD pathology, since AD is also associated with synaptic loss, and the observed differences here were not present in the WT animals.

As mentioned before, female APP mice show a higher A β burden than their male counterparts, as shown both in the ELISA analyses and the immunohistochemical staining. This indicates a heavier AD pathology in female mice. Important to note, the A β burden is just a marker for AD, it is not a direct comparison for AD pathology. The exact contribution of the A β plaques to AD pathology remains unclear, but it is known that there are correlations between the amount of A β plaques and other factors associated with AD (Hooijmans et al., 2007). Hooijmans et al. demonstrated that A β plaques are related to decreased GLUT-1 and hippocampal atrophy in 18-month-old mice (Hooijmans et al., 2007) and both A β plaques and AD directly affect synaptic density negatively (Goulay, Romo, Hol, & Dijkhuizen, 2019; Dennis J Selkoe, 2002). Taken all together, a cautious link can be made to the high of A β burden and the overall weight of the AD pathology. Therefore, a more severe AD pathology indicated by a higher A β burden could explain the reduction in synaptic density in female mice, since AD negatively affects the synapses.

It would be beneficial to look at other AD markers such as vascularity and neuroinflammation

that may also differ between sexes to confirm the correlation between the synaptic density and heavier AD pathology. This could shed light on the question whether the observed effect is solely driven by A β burden or by the overall AD pathology.

Future perspective

Longitudinal studies on the combination of AD and stroke have never been done before. This study is the first step to elucidate the long-term effects of stroke on AD pathology. Both the AD and stroke model have been widely used in research and have also been combined to determine short-term effects of stroke and AD on each other. There are some considerations to be made for the stroke model and its controls, both within and between subjects. Especially, differences of the two control models should be closely considered for their implications. Both controls can be influenced by the surgeries done, and it is vital to keep this in mind when comparing experimental groups.

To investigate the effect of sex, both male and female mice were used. In humans, females are protected via estrogen against the development, as well as the severe adverse effects of stroke (Reeves et al., 2008). Therefore, postmenopausal women are more prone to suffer a stroke. The current mouse model does not take this postmenopausal group into account. Future research could benefit from including groups that represent both pre- and postmenopausal women.

The mice used in this study also underwent multiple other tests, including behavioral studies and MRI analyses. It was not possible to include all data in this report. However, correlation analyses between behavioral studies, MRI data and postmortem analysis are crucial to elucidate the overall effect of stroke on AD. Markers for neuronal and synaptic density could be correlated to previously performed cognitive test results. Also, neuroinflammatory factors should be correlated to A β burden. Originally, neurogenesis was planned to be further investigated by means of qPCR analysis of BDNF mRNA expression. However, due to the age of the mice and the low level of DCX-positive cells found in the hippocampus (other data from current study, not published yet), the concentrations were too low to be properly analyzed.

A crucial factor in AD pathology is the vascularity of the brain. GLUT-1 transporters in the blood vessels are vital for A β clearance in the brain (Ueno et al., 2014) and most AD patients show vascular pathologies postmortem (R. N. Kalaria et al., 2012).

A previous study already found a correlation between GLUT-1 and A β plaques in the mouse model that was used in the current study (Hooijmans et al., 2007). Postmortem analyses of GLUT-1 and overall architecture of the vascularity should be done and correlated to A β burden, MRI data and behavioral test.

Lastly, cell death should be considered as an influencing factor. By looking at the immunohistochemical staining, cell death and atrophy were seen in the basal ganglia, however, the full extent of this atrophy should be further analyzed by MRI. The degree of atrophy could also be correlated to the behavioral tests, especially focusing on memory tests and e.g. hippocampal atrophy. Overall, many factors are still to be considered in future research.

Conclusions

Due to the growing life expectancy, AD and stroke prevalence are expected to rise even more in the coming years (Association, 2019). Studies on the direct interaction but also the long-term effects of stroke and AD are important to improve treatment of the conditions and eventually reduce the prevalence of both. Sex is an important factor in many diseases and disorders, including AD and stroke. Therefore, including both sexes in research is vital for understanding the different presentation of the disorders.

The current longitudinal study replicated the sex differences found in A β plaques in the hippocampus and showed that this increased A β burden in females also extends to other brain areas such as the thalamus and basal ganglia. Eight months after stroke induction male mice showed a decrease in A β plaques in the areas directly affected by the stroke compared to the unaffected hemisphere, possibly due to increased microglial activity in the affected hemisphere. This effect of microglial activity between the two hemispheres was not present in the female mice. Differences between male and female mice were also present in synaptic density, specifically in asymmetrical expression between hemispheres. Furthermore, female APP mice showed an overall lower synaptic density than their male counterpart. This is most likely caused by the increased A β pathology in the female mice. Overall, the effects of stroke on AD are profound, but varying between the sexes. More research on AD pathological markers other than A β burden and synaptic density should shed more light on the long-term effects of stroke on AD.

References

- Agüero-Torres, H., Kivipelto, M., & von Strauss, E. (2006). Rethinking the dementia diagnoses in a population-based study: what is Alzheimer's disease and what is vascular dementia? *Dementia and Geriatric Cognitive Disorders*, 22(3), 244-249.
- Amarenco, P., Bogousslavsky, J., Caplan, L., Donnan, G., & Hennerici, M. (2009). Classification of stroke subtypes. *Cerebrovascular diseases*, 27(5), 493-501.
- Appelros, P., Stegmayr, B., & Terént, A. (2009). Sex differences in stroke epidemiology: a systematic review. *Stroke*, 40(4), 1082-1090.
- Association, A. s. (2019). 2019 Alzheimer's disease facts and figures. *Alzheimer's & Dementia*, 15(3), 321-387.
- Azad, N. A., Al Bugami, M., & Loy-English, I. (2007). Gender differences in dementia risk factors. *Gender medicine*, 4(2), 120-129.
- Bertrand, L., Dygert, L., & Toborek, M. (2017). Induction of ischemic stroke and ischemia-reperfusion in mice using the middle artery occlusion technique and visualization of infarct area. *JoVE (Journal of Visualized Experiments)*(120), e54805.
- Cacace, R., Slegers, K., & Van Broeckhoven, C. (2016). Molecular genetics of early-onset Alzheimer's disease revisited. *Alzheimer's & Dementia*, 12(6), 733-748.
- Callahan, M. J., Lipinski, W. J., Bian, F., Durham, R. A., Pack, A., & Walker, L. C. (2001). Augmented senile plaque load in aged female β -amyloid precursor protein-transgenic mice. *The American journal of pathology*, 158(3), 1173-1177.
- Chi, N.-F., Chien, L.-N., Ku, H.-L., Hu, C.-J., & Chiou, H.-Y. (2013). Alzheimer disease and risk of stroke: a population-based cohort study. *Neurology*, 80(8), 705-711.
- de Bruijn, R. F., & Ikram, M. A. (2014). Cardiovascular risk factors and future risk of Alzheimer's disease. *BMC medicine*, 12(1), 130.
- de la Torre, J. C. (2004). Is Alzheimer's disease a neurodegenerative or a vascular disorder? Data, dogma, and dialectics. *The Lancet Neurology*, 3(3), 184-190.
- De Reuck, J. (1971). The human periventricular arterial blood supply and the anatomy of cerebral infarctions. *European neurology*, 5(6), 321-334.
- DeKosky S.T., S. S. W., and Styren S.D. (1996). Structural correlates of cognition in dementia: quantification and assessment of synapse change. *Neurodegener J Neurodegener Disord Neuroprotection Neuroregeneration*, 5, 417-421.
- Drouin, E., & Drouin, G. (2017). The first report of Alzheimer's disease. *The Lancet Neurology*, 16(9), 687.
- Eckenhoff, R. G., Johansson, J. S., Wei, H., Carnini, A., Kang, B., Wei, W., . . . Eckenhoff, M. F. (2004). Inhaled anesthetic enhancement of amyloid- β oligomerization and cytotoxicity. *Anesthesiology: The Journal of the American Society of Anesthesiologists*, 101(3), 703-709.
- Garcia-Alloza, M., Gregory, J., Kuchibhotla, K. V., Fine, S., Wei, Y., Ayata, C., . . . Bacskai, B. J. (2011). Cerebrovascular lesions induce transient β -amyloid deposition. *Brain*, 134(12), 3697-3707.
- Goedert, M., & Spillantini, M. G. (2006). A century of Alzheimer's disease. *Science*, 314(5800), 777-781.
- Goodwin, L. O., Splinter, E., Davis, T. L., Urban, R., He, H., Braun, R. E., . . . Ndukum, J. (2019). Large-scale discovery of mouse transgenic integration sites reveals frequent structural variation and insertional mutagenesis. *Genome research*, 29(3), 494-505.
- Goulay, R., Romo, L. M., Hol, E. M., & Dijkhuizen, R. M. (2019). From Stroke to Dementia: a Comprehensive Review Exposing Tight Interactions Between Stroke and Amyloid- β Formation. *Translational stroke research*, 1-14.
- Gouras, G. K., Tsai, J., Naslund, J., Vincent, B., Edgar, M., Checler, F., . . . Xu, H. (2000). Intraneuronal A β 42 accumulation in human brain. *The American journal of pathology*, 156(1), 15-20.
- Haast, R. A., Gustafson, D. R., & Kiliaan, A. J. (2012). Sex differences in stroke. *Journal of Cerebral Blood Flow & Metabolism*, 32(12), 2100-2107.
- Han, B., Wang, J.-H., Geng, Y., Shen, L., Wang, H.-L., Wang, Y.-Y., & Wang, M.-W. (2017). Chronic stress contributes to cognitive dysfunction and hippocampal metabolic abnormalities in APP/PS1 mice. *Cellular Physiology and Biochemistry*, 41(5), 1766-1776.
- Holtzman, D. M., Bales, K. R., Tenkova, T., Fagan, A. M., Parsadanian, M., Sartorius, L. J., . . . Wozniak, D. (2000). Apolipoprotein E isoform-dependent amyloid deposition and neuritic degeneration in a mouse model of Alzheimer's disease. *Proceedings of the National Academy of Sciences*, 97(6), 2892-2897.
- Honig, L. S., Tang, M.-X., Albert, S., Costa, R., Luchsinger, J., Manly, J., . . . Mayeux, R. (2003). Stroke and the risk of Alzheimer disease. *Archives of neurology*, 60(12), 1707-1712.
- Hooijmans, C. R., Graven, C., Dederen, P. J., Tanila, H., van Groen, T., & Kiliaan, A. J. (2007). Amyloid beta deposition is related to decreased glucose transporter-1 levels and hippocampal atrophy in brains of aged APP/PS1 mice. *Brain research*, 1181, 93-103.
- Huang, H., Wang, L., Cao, M., Marshall, C., Gao, J., Xiao, N., . . . Xiao, M. (2015). Isolation housing exacerbates Alzheimer's disease-like pathophysiology in aged APP/PS1 mice. *International Journal of Neuropsychopharmacology*, 18(7), pyu116.
- Jankowsky, J. L., Fadale, D. J., Anderson, J., Xu, G. M., Gonzales, V., Jenkins, N. A., . . . Wagner, S. L. (2003). Mutant presenilins specifically elevate the levels of the 42 residue β -amyloid peptide in vivo: evidence for augmentation of a 42-specific γ secretase. *Human molecular genetics*, 13(2), 159-170.
- Jankowsky, J. L., Slunt, H. H., Ratovitski, T., Jenkins, N. A., Copeland, N. G., & Borchelt, D. R. (2001). Co-expression of multiple transgenes in mouse CNS: a comparison of strategies. *Biomolecular engineering*, 17(6), 157-165.
- Jarrett, J. T., Berger, E. P., & Lansbury Jr, P. T. (1993). The carboxy terminus of the beta. amyloid protein

- is critical for the seeding of amyloid formation: Implications for the pathogenesis of Alzheimer's disease. *Biochemistry*, 32(18), 4693-4697.
- Jendroska, K., Hoffmann, O., & Patt, S. (1997). Amyloid β peptide and precursor protein (APP) in mild and severe brain ischemia. *Annals of the New York Academy of Sciences*, 826(1), 401-405.
- Jendroska, K., Poewe, W., Pluess, J., Iwerssen-Schmidt, H., Paulsen, J., Barthel, S., . . . DeArmond, S. (1995). Ischemic stress induces deposition of amyloid β immunoreactivity in human brain. *Acta neuropathologica*, 90(5), 461-466.
- Kalaria, R. (2002). Similarities between Alzheimer's disease and vascular dementia. *Journal of the neurological sciences*, 203, 29-34.
- Kalaria, R. N., Akinyemi, R., & Ihara, M. (2012). Does vascular pathology contribute to Alzheimer changes? *Journal of the neurological sciences*, 322(1-2), 141-147.
- Kemppainen, S., Hämäläinen, E., Miettinen, P., Koistinaho, J., & Tanila, H. (2014). Behavioral and neuropathological consequences of transient global ischemia in APP/PS1 Alzheimer model mice. *Behavioural brain research*, 275, 15-26.
- Kim, J.-S., Lee, K.-B., Roh, H., Ahn, M.-Y., & Hwang, H.-W. (2010). Gender differences in the functional recovery after acute stroke. *Journal of Clinical Neurology*, 6(4), 183-188.
- Kivipelto, M., Helkala, E.-L., Laakso, M. P., Hänninen, T., Hallikainen, M., Alhainen, K., . . . Nissinen, A. (2001). Midlife vascular risk factors and Alzheimer's disease in later life: longitudinal, population based study. *Bmj*, 322(7300), 1447-1451.
- Klyubin, I., Cullen, W. K., Hu, N.-W., & Rowan, M. J. (2012). Alzheimer's disease A β assemblies mediating rapid disruption of synaptic plasticity and memory. *Molecular brain*, 5(1), 25.
- Launer, L., Andersen, K., Dewey, M., Letenneur, L., Ott, A., Amaducci, L., . . . Kragh-Sorensen, P. (1999). Rates and risk factors for dementia and Alzheimer's disease: results from EURODEM pooled analyses. *Neurology*, 52(1), 78-78.
- Lewis, H., Beher, D., Cookson, N., Oakley, A., Piggott, M., Morris, C., . . . Kenny, R. (2006). Quantification of Alzheimer pathology in ageing and dementia: age-related accumulation of amyloid- β (42) peptide in vascular dementia. *Neuropathology and applied neurobiology*, 32(2), 103-118.
- Leys, D., Erkinjuntti, T., Desmond, D. W., Schmidt, R., Englund, E., Pasquier, F., . . . Chabriat, H. (1999). Vascular dementia: the role of cerebral infarcts. *Alzheimer disease and associated disorders*, 13, S38-48.
- Marchal, G., Beaudouin, V., Rioux, P., de la Sayette, V., Le Doze, F. o., Viader, F., . . . Baron, J. C. (1996). Prolonged persistence of substantial volumes of potentially viable brain tissue after stroke: a correlative PET-CT study with voxel-based data analysis. *Stroke*, 27(4), 599-606.
- Marques, A. F. V. d. S., & Lapa, T. A. S. C. (2018). Anesthesia and Alzheimer disease—Current perceptions. *Revista brasileira de anesthesiologia*, 68(2), 174-182.
- McGowan, E., Pickford, F., Kim, J., Onstead, L., Eriksen, J., Yu, C., . . . Das, P. (2005). A β 42 is essential for parenchymal and vascular amyloid deposition in mice. *Neuron*, 47(2), 191-199.
- Merlo, S., Spampinato, S., Caruso, G., & Sortino, M. (2020). The ambiguous role of microglia in A β toxicity: Chances for therapeutic intervention. *Current neuropharmacology*.
- Nakamura, Y., Takeda, M., Niigawa, H., Hariguchi, S., & Nishimura, T. (1992). Amyloid β -protein precursor deposition in rat hippocampus lesioned by ibotenic acid injection. *Neuroscience letters*, 136(1), 95-98.
- Nelson, A. R., Sweeney, M. D., Sagare, A. P., & Zlokovic, B. V. (2016). Neurovascular dysfunction and neurodegeneration in dementia and Alzheimer's disease. *Biochimica et Biophysica Acta (BBA)-Molecular Basis of Disease*, 1862(5), 887-900.
- Ordóñez-Gutiérrez, L., Antón, M., & Wandosell, F. (2015). Peripheral amyloid levels present gender differences associated with aging in A β PP/PS1 mice. *Journal of Alzheimer's Disease*, 44(4), 1063-1068.
- Radde, R., Bolmont, T., Kaeser, S. A., Coomaraswamy, J., Lindau, D., Stoltze, L., . . . Gengler, S. (2006). A β 42-driven cerebral amyloidosis in transgenic mice reveals early and robust pathology. *EMBO reports*, 7(9), 940-946.
- Ramanathan, A., Nelson, A. R., Sagare, A. P., & Zlokovic, B. V. (2015). Impaired vascular-mediated clearance of brain amyloid beta in Alzheimer's disease: the role, regulation and restoration of LRP1. *Frontiers in aging neuroscience*, 7, 136.
- Reeves, M. J., Bushnell, C. D., Howard, G., Gargano, J. W., Duncan, P. W., Lynch, G., . . . Lisabeth, L. (2008). Sex differences in stroke: epidemiology, clinical presentation, medical care, and outcomes. *The Lancet Neurology*, 7(10), 915-926.
- Robinson, J. L., Molina-Porcel, L., Corrada, M. M., Raible, K., Lee, E. B., Lee, V. M.-Y., . . . Trojanowski, J. Q. (2014). Perforant path synaptic loss correlates with cognitive impairment and Alzheimer's disease in the oldest-old. *Brain*, 137(9), 2578-2587.
- Roger, V. L., Go, A. S., Lloyd-Jones, D. M., Adams, R. J., Berry, J. D., Brown, T. M., . . . Ford, E. S. (2011). Heart disease and stroke statistics—2011 update: a report from the American Heart Association. *Circulation*, 123(4), e18-e209.
- Roy, S., Nag, T. C., Upadhyay, A. D., Mathur, R., & Jain, S. (2014). Prenatal music stimulation facilitates the postnatal functional development of the auditory as well as visual system in chicks (*Gallus domesticus*). *Journal of biosciences*, 39(1), 107-117.
- Sahathevan, R., Brodtmann, A., & Donnan, G. A. (2012). Dementia, stroke, and vascular risk factors; a review. *International Journal of Stroke*, 7(1), 61-73.
- Selkoe, D. J. (2002). Alzheimer's disease is a synaptic failure. *Science*, 298(5594), 789-791.
- Selkoe, D. J., & Schenk, D. (2003). Alzheimer's disease: molecular understanding predicts amyloid-based

- therapeutics. *Annu Rev Pharmacol Toxicol*, 43, 545-584. doi:10.1146/annurev.pharmtox.43.100901.140248
- Shankar, G. M., & Walsh, D. M. (2009). Alzheimer's disease: synaptic dysfunction and A β . *Molecular neurodegeneration*, 4(1), 48.
- Sherwood, C. C., Duka, T., Stimpson, C. D., Schenker, N. M., Garrison, A. R., Schapiro, S. J., . . . Hof, P. R. (2010). Neocortical synaptophysin asymmetry and behavioral lateralization in chimpanzees (Pan troglodytes). *European Journal of Neuroscience*, 31(8), 1456-1464.
- Simões, A. E., Pereira, D. M., Amaral, J. D., Nunes, A. F., Gomes, S. E., Rodrigues, P. M., . . . Thibodeau, S. N. (2013). Efficient recovery of proteins from multiple source samples after trizol® or trizol® LS RNA extraction and long-term storage. *BMC genomics*, 14(1), 181.
- Skoog, I., Nilsson, L., Persson, G., Lernfelt, B., Landahl, S., Palmertz, B., . . . Svanborg, A. (1996). 15-year longitudinal study of blood pressure and dementia. *The Lancet*, 347(9009), 1141-1145.
- Sun, X., He, G., Qing, H., Zhou, W., Dobie, F., Cai, F., . . . Song, W. (2006). Hypoxia facilitates Alzheimer's disease pathogenesis by up-regulating BACE1 gene expression. *Proceedings of the National Academy of Sciences*, 103(49), 18727-18732.
- Sweeney, M. D., Sagare, A. P., & Zlokovic, B. V. (2015). Cerebrospinal fluid biomarkers of neurovascular dysfunction in mild dementia and Alzheimer's disease. *Journal of Cerebral Blood Flow & Metabolism*, 35(7), 1055-1068.
- Thiel, A., Cechetto, D. F., Heiss, W.-D., Hachinski, V., & Whitehead, S. N. (2014). Amyloid burden, neuroinflammation, and links to cognitive decline after ischemic stroke. *Stroke*, 45(9), 2825-2829.
- Ueno, M., Chiba, Y., Matsumoto, K., Nakagawa, T., & Miyanaka, H. (2014). Clearance of beta-amyloid in the brain. *Current medicinal chemistry*, 21(35), 4085-4090.
- Vallortigara, G., Chiandetti, C., & Sovrano, V. A. (2011). Brain asymmetry (animal). *Wiley Interdisciplinary Reviews: Cognitive Science*, 2(2), 146-157.
- Wang, J., Tanila, H., Puoliväli, J., Kadish, I., & van Groen, T. (2003). Gender differences in the amount and deposition of amyloid β in APPswe and PS1 double transgenic mice. *Neurobiology of disease*, 14(3), 318-327.
- Waters, N. S., & Denenberg, V. H. (1994). Analysis of two measures of paw preference in a large population of inbred mice. *Behavioural Brain Research*, 63(2), 195-204.
- White, L., Petrovitch, H., Hardman, J., Nelson, J., Davis, D. G., Ross, G. W., . . . Markesbery, W. R. (2002). Cerebrovascular pathology and dementia in autopsied Honolulu-Asia Aging Study participants. *Annals of the New York Academy of Sciences*, 977(1), 9-23.
- Wuwongse, S., Cheng, S. S.-Y., Wong, G. T.-H., Hung, C. H.-L., Zhang, N. Q., Ho, Y.-S., . . . Chang, R. C.-C. (2013). Effects of corticosterone and amyloid-beta on proteins essential for synaptic function: implications for depression and Alzheimer's disease. *Biochimica et Biophysica Acta (BBA)-Molecular Basis of Disease*, 1832(12), 2245-2256.
- Zeng, Y., Zhang, J., Zhu, Y., Zhang, J., Shen, H., Lu, J., . . . Zhou, M. (2015). Tripchlorolide improves cognitive deficits by reducing amyloid β and upregulating synapse-related proteins in a transgenic model of Alzheimer's Disease. *Journal of neurochemistry*, 133(1), 38-52.

Supplementary information

Supplementary protocol 1: RNA isolation

The protocol is done in the fume hood. Always wear gloves and clean them regularly with 70% ethanol. Make sure that there are enough sterile pipette tips and autoclaved 1,5 ml Eppendorf tubes, and enough DEPC-treated milliQ, TRIzol, chloroform, and 2-propanol and 75% ethanol. All pipette tips and tubes that have come into contact with TRIzol have to be collected in a glass container and disposed of in the chemical waste container. The protocol is used to isolate RNA from frozen (-80°) tissue, which is placed in a 2 ml Eppendorf tube. The tubes with MQ and ethanol used for cleaning the homogenizer and the 2-propanol and ethanol supernatants from steps 24 and 28 need to be collected in a 50 ml tube and disposed of in the chemical waste container.

1. Switch on the centrifuge, set it to 4°. Get a bucket of ice. Place the tissue homogeniser in the fume hood. Switch on the thermomixer and set it to 60°.

For each 4 samples you have, fill one marked test tube half full with 70% ethanol and one marked test tube half full with MQ (DEPC-treated).

2. Take the tissue samples from the freezer and put them in the ice bucket

3. In the fume hood, add 1 ml of TRIzol to each sample

4. Dip the tip of the homogenizer into the test tube with 70% ethanol

5. Clean the tip of the homogenizer with a tissue paper

6. Put the homogenizer into the tube with TRIzol and your sample, push the tissue down, switch on the homogenizer for 10 seconds, move the tube up and down during the homogenizing

7. Close the tube and put it back in the ice

8. Put the homogenizer into the test tube with MQ and switch on the machine for about 3 seconds

Clean the tip of the homogenizer with a tissue paper

Dip the tip of the homogenizer into the test tube with 70% EtOH

Clean the tip of the homogenizer with a tissue paper

9. Homogenize the next sample (steps 6-8)

10. Switch to new test tubes with MQ and EtOH, and tissue paper, after each 4 samples

11. Store the samples at RT for 5 minutes

12. Add 200 µl of chloroform to each sample

13. Shake the tubes vigorously for 15 seconds

14. Store the samples at RT for 5 minutes

15. Centrifuge at 12.000 g at 4° for 10 minutes

16. Make a new labeled, sterile 1,5 ml Eppendorf tube for each sample

17. Carefully put the centrifuged tubes back into the ice

18. In the fume hood, pipette the top, clear layer (500 µl) into the new tube. Be careful not to touch the intermediate layer with your pipette tip.

It's more important that what you pipette off is clean than that you get the whole 500 µl

19. Add 500 µl of 2-propanol to each tube

20. Shake the tubes vigorously for 15 seconds

21. Store the samples at RT for 15 minutes

22. Centrifuge at 12.000 g at 4° for 10 minutes

23. Carefully put the tubes back into the ice. Most of the times, a white pellet is visible at the bottom of the tube

24. Set the pipette to 600 µl, and carefully pipette off the supernatant in two steps. Do not touch the pellet or the place where the pellet should be. Discard the supernatant into the 50 ml tube

25. Add 1 ml of 75% EtOH to each tube. Flick the tubes

26. Centrifuge at 7.500 g at 4° for 5 minutes

27. Carefully put the tubes back into the ice

28. Set the pipette to 600 µl, and carefully pipette off the supernatant in two steps. Do not touch the pellet or the place where the pellet should be. Discard the supernatant into the 50 ml tube. Set another pipette to 50 µl and pipette out the last remaining ethanol

29. Take the tubes out of the ice, open the tubes and let the RNA dry for 10 minutes

30. Add 25 µl of MQ (DEPC-treated) to each sample. Pipette up and down a few times

31. Put the tubes in the thermomixer (no shaking) for 10 minutes

32. Flick the tubes with your fingers and spin them down

33. Store the tubes at -80°C or continue with the protocol for measuring the RNA concentration using the NanoDrop

Supplementary protocol 2: Measuring RNA/DNA with the Nanodrop 2000

Using this protocol, you can measure the concentration and purity of your RNA or DNA samples, using the NanoDrop spectrophotometer.

Many proteins absorb at 280 (aromatic rings

absorb this wavelength) and DNA/RNA absorbs at 260. 260/280 ratio should be 1.80-2.00, 260/230 1.80-2.20. When working with RNA isolated with TRIzol, the 260/230 values are going to be lower (0.3-0.8) because of the high salt concentrations.

1. Switch on the computer and screen. The NanoDrop machine is always on. When working with RNA, get a bucket of ice, and wear clean gloves throughout the protocol

2. Thaw your samples (if needed)

3. Flick your samples using your fingers, spin them down

4. When working with RNA, put your samples on ice

5. Run the NanoDrop 2000 program on the computer

6. Select 'Nucleic acids' on the menu screen

7. Make sure the arm of the NanoDrop is down, click OK

8. In the top right corner of the screen, select if you want to measure DNA or RNA

9. Pipette 1 μ l of the solution your DNA or RNA is dissolved in (usually 1x TE or DEPC-MQ) onto the pedestal, put the arm down, and click the 'Blank' button in the program

10. Put the arm up when the blank measurement is done and, using a tissue paper, gently wipe off the liquid from the pedestal and the arm

11. Pipette 1 μ l of your DNA/RNA sample onto the pedestal, put the arm down, fill in your sample number in the field in the top right, and click the 'Measure' button in the program

12. Put the arm up when the measurement is done and, using a tissue paper, gently wipe off the liquid from the pedestal and the arm

13. When working with RNA, measure your sample again (duplo) with a new 1 μ l

14. Repeat steps 11-13 for all your samples

15. After the first sample, you get a pop-up asking you where you want to save your data

16. After the last sample is measured, click the 'Reports' button in the lower left corner of the screen. Click 'Export' to export your data to an .xml file you can use later on

17. Close the NanoDrop program and switch off the computer and screen

18. Store the tubes at -80°C or continue with the next protocol

Supplementary protocol 3: DNA treatment of RNA

Get a bucket of ice. Thaw the RNA samples (if

needed). Flick them and spin them down and put them on ice. Get the DNase, DNase buffer, and DNase stop solution from the -20° freezer. Set the Thermomixer to 37°C (no shaking). All steps are done on ice, unless stated otherwise.

1. Take an autoclaved Eppendorf vial (1,5 ml) for each RNA sample and label it.

2. Add up to 1 μ g of RNA to the vial, add MQ to 8 μ l.

3. Add 1 μ l of DNase buffer to each vial.

4. Add 1 μ l of DNase enzyme to each vial.

5. Flick the tubes, spin them down.

6. Put the vials in the 37° Thermomixer for 30 minutes.

7. Take the tubes out of the Thermomixer, put them back on ice. Set the Thermomixer to 65° .

8. Add 1 μ l of Stop solution to each vial.

9. Flick the tubes, spin them down.

10. Put the vials in the 65° Thermomixer for 10 minutes.

11. Take the tubes out of the Thermomixer, put them back on ice.

12. Measure the RNA concentration with the NanoDrop and store the RNA in the -80° freezer.

Supplementary protocol 4: cDNA synthesis

This protocol can be used to generate cDNA from RNA. The main idea is that one absolute amount of RNA is added to the cDNA synthesis reaction and that this amount is the same for all the samples. The preparation that needs to be done for this protocol is that for all your samples you have to calculate how many μ l of RNA you have to add to the reaction mix to get the absolute amount. The equation for calculating how many μ l you have to add is

$$\frac{\text{(absolute amount you want)}}{\text{(RNA concentration of the sample)}}$$

The reaction mix per sample consists of:

- x μ l RNA
- (7.5 - x) μ l of RNase-free water
- 2 μ l of 5x reverse transcription reaction mix
- 0.5 μ l of reverse transcriptase enzyme

So, the maximum volume of RNA that can be added is 7.5 μ l. Calculate the absolute amount of RNA you want to add based on the sample in your collection with the lowest RNA

concentration.

The maximum amount of RNA that can be added to this 10 μl reaction is 500 ng.

1. Calculate how many μl of RNA you need to pipette to get the absolute amount of RNA (400 ng), and calculate how many μl of RNase-free water you need to add to that to get to 7.5 μl end volume.
2. Get a bucket of ice
3. Thaw your RNA samples and the 5x reverse transcription reaction mix, flick them with your fingers and put them in the ice
4. Put the reverse transcriptase enzyme directly on ice, it is not frozen
5. Prepare 8-tubestrips
6. Add the RNase-free water to the strips, then the RNA. The total volume in each tube should be 7.5 μl
7. Add 2 μl of 5x reverse transcription reaction mix to each tube, then add 0.5 μl reverse transcriptase enzyme
8. Close the tubestrips, flick them with your finger and spin them down
9. Put the strips in the PCR machine and run the ISCRIP program
10. Spin the strips down and dilute the cDNA 1:10 using MQ. Tap the strips to mix
11. Spin the strips down, store them at 4° (short term) or -20° (long term)

Supplementary protocol 5: qPCR

Use this protocol to prepare a QPCR plate, configure the ABI Prism 7900HT or StepOne Plus machine, and run the QPCR protocol. Read up on the background & principles of QPCR using the attached qRT-PCR_Basics PDF file. We use the SYBR Green method here. To make the QPCR master mix (see below), use the Bio-Rad iTaq SYBR Green mix. Use the MicroAmp Optical 96-Well plates. To make the QPCR master mix (see below), use the Bio-Rad iTaq SYBR Green mix. Use the MicroAmp Fast 96-Well plates.

First, design the layout of the QPCR plate. All samples must be run in triplicates, so select three adjacent wells for each sample. Three wells are used for the no template control (NTC), a reaction in which MQ will be added instead of a sample. This NTC is used to check whether no cDNA contamination is present in the QPCR master mix.

If you have multiple primer sets in one plate, make a master mix for each pair. Calculate how much master mix you need to make ((number of samples + 1 NTC) x 3). Because of pipette errors and dead

volumes of pipettes, make some extra master mix. When you have 24 samples, add 3 samples.

For each well you need these components:

- 5 μl SYBR Green mix (Bio-Rad iTaq)
- 0.4 μl forward primer
- 0.4 μl reverse primer
- 2.2 μl MQ

This is 8 μl in total.

1. Get a bucket of ice.
2. Made the mix in reverse order, so add the SYBR Green mix last. When pipetting this, pipette a few times up and down to mix everything. Master mixes cannot be vortexed. Put the master mixes on ice. Defrost the cDNA (if needed), flick the strips and spin them down. They can be kept at room temperature.
3. Get a plate, put it in a black plate holder (base plate) and put it on ice.
4. Use a manual pipette set to 8.0 μl or the electric repeater pipette set to 8.0 μl aliquots to pipette the master mix into the plate.
5. Use the manual P2 pipette to add 2 μl of cDNA to the correct wells. Add 2 μl of MQ to the NTC wells.
6. Take the plate out of the ice.
7. Affix a cover sticker to the plate, using the gray applicator. Press down the sticker on all sides and corners. Use your fingers to press down the sticker on each well. Spin down the plate using the plate spinner.
8. Take your plate to the StepOne Plus. Switch on the machine and the computer
9. Designing the plate is done on your own zero client. Then you save this and take it to the QPCR machine to run it
10. Start StepOne Software v2.3
11. Click OK
12. Click File -> New Experiment -> Advanced Setup
13. Fill in Experiment Name and Username
14. Click SYBR Green Reagents button & Standard (~ 2 hours to complete a run) buttons
15. Click the Plate Setup button in the top left of the screen
16. Fill in the target name (the name of your gene of interest). If there are more than 1 on your plate, click Add New Target
17. Fill in the names of the samples. Click Add New Sample button for each sample. Also add the NTC as a sample
18. Click the Assign Targets and Samples button
19. Design the plate layout according to your

scheme, selecting the appropriate Target and Sample for each well. When selecting the NTC, click the N button under Task. All other samples are set to U.

20. Click the Run Method button in the top left of the screen

21. Change the first step to 30 seconds 95° instead of 10 minutes. First change the seconds to 30, then change the minutes to 00

22. Change Reaction Volume Per Well to 10

23. In the top left of the screen, click the save icon and save your file on your USB stick

24. Take the plate and the USB stick to the StepOnePlus machine at Internal Medicine

25. Switch on the computer if necessary

26. Put your USB stick in the computer, copy your .eds file to the Anatomy folder in the Users folder (located on the desktop)

27. Start the StepOne Software

28. Open the tray of the StepOnePlus machine, put your plate in and close the tray

29. In the top left of the screen, click the Open button and find your file in the Users -> Anatomy folder. Open it

30. Click the START RUN button in the top right corner of the screen

31. After about 2 hours the run is done

32. Click the Save button

33. Open the tray of the machine and remove the plate. Close the tray

34. Copy the .eds file to your USB stick

35. Close the StepOne software

36. Open the .eds file on your zero client

37. Uncheck the Auto box next to Threshold in the bottom of the screen

38. Fill in 0.2 and press Enter

39. Click the Export button in the top of the screen

40. Click the Customize Export tab

41. Uncheck everything except Well, Sample Name, Target Name, Task, Ct, Ct Threshold, Tm1, Tm2, Tm3

42. Click the Export Properties tab

43. Change the Export File Location to your folder

44. Check the Open file(s) when export is complete box

45. Click the Start Export button

46. Do data analyses in Excel

Supplementary protocol 6: gDNA isolation with Trizol

Step 1 to 18 from the RNA isolation protocol

(Labguru, Bram Geenen),

1. Pipette off the RNA phase

2. Add 500 µl 100% Ethanol to the phenol and interphase of the sample

3. Carefully shake until you see the DNA appear

4. Centrifuge at 7.500g for 5 minutes at RT

5. Discard supernatant (with pipette)

6. Add 700 µl Sodium citrate in 10% Ethanol, pH 8,5

7. Wash pellet by carefully moving the tube upside down a few times

8. Centrifuge at 7.500g for 5 minutes at RT

9. Discard supernatant (with pipette)

10. Add 700 µl 70% Ethanol

11. Wash pellet by carefully moving the tube upside down a few times

12. Centrifuge at 7.500g for 5 minutes at RT

13. Discard supernatant (with pipette)

14. Let the pellet dry for ca. 10 minutes

15. Add 500 µl MQ

16. Vortex and spin tubes down

17. Measure gDNA with Nanodrop with the 'Measuring RNA/DNA with the NanoDrop 2000' protocol (Labguru, Bram Geenen)

18. Samples are stored at -20°C until further analysis will be performed

Note: concentration of the DNA has to be below 100 ng/µl for successful genotyping. Dilute if needed.

Sodium citrate:

1. Dissolve 1.455 g sodium citrate (2 H₂O) in 5 ml 100% ethanol

2. Add MQ to a total of 40 ml

3. Adjust pH to 8,5

4. Add MQ to a total of 50 ml

Supplementary protocol 7: running a agarose gel

1. Set up the gelelectrophoresis system

2. Combine 100 ml of 1x TBE and 1.0 gram of agarose powder in a medium flask.

3. Mix gently.

4. Microwave on HIGH until the mixture starts to boil. Gently mix the contents. Beware of delayed boiling! Repeat another 2 times until agarose is completely dissolved.

5. Allow the contents in the flask to cool until it stops steaming.

6. Avoid introducing any additional air bubbles.

7. Add 10 μ l of SYBR Safe DNA stain to the flask using a pipette.
8. Mix gently and carefully pour gel.
9. Remove any air bubbles in gel lanes by gently pushing the bubbles off to the sides with pipette tip.
10. Allow gel to harden at RT for 20 minutes
11. Put gel and TBE buffer in agarose system.
12. Add 5 μ l of loading buffer to each sample.
13. Load 5 μ l of TrackIt 100 bp ladder into the first slot.
14. Carefully inject 5 μ l of each sample into the slots in the gel.
15. Run gel at 100V. for 30 minutes
16. Take a picture of the gel using the GelDoc
15. Repeat step 6 step 9 twice (wash three times in total)
16. Air dry the protein pellet for 5–10 minutes
17. Add a tablet Complete protease inhibitor to 10 ml of 5M Guanidine buffer
18. Resuspend the pellet in 500 μ L of 5M guanidine hydrochloride in Tris-HCl, pH8) by pipetting up and down
19. Vortex to complete suspension
20. Centrifuge for 10 minutes at $10,000 \times g$ at 4°C to remove insoluble materials
21. Transfer the supernatant to a new 1.5 ml tube (Guanidine Soluble Fraction)
22. Samples are stored at -80°C until the ELISA will be performed

Solutions:

- Invitrogen SYBR Safe DNA Gel Stain (400 μ l) Life Technologies #S33102
- Invitrogen TrackIt 100 bp ladder (500 μ l) Life Technologies #10488-058
- Invitrogen UltraPure™ TBE Buffer, 10X (1 L) Life Technologies #15581-044
- Invitrogen UltraPure™ Agarose (100 gram) Life Technologies #16500-100

0.3M Guanidine buffer:

Dissolve 7.164 gr guanidine HCl in 250ml 95ml Ethanol.

5M Guanidine buffer:

Dissolve 119.4 gr guanidine HCl and 1.5 gr Trizma base in 200 ml MQ
Adjust pH to 8.0
Add MQ to a total of 250 ml (expiration date 2 years)

Supplementary protocol 8: Protein isolation

Day 1 RNA isolation

1. Step 1 to 18 from the RNA isolation protocol (Labguru, Bram Geenen)

Day 2 DNA en Protein isolation o/n 4°C

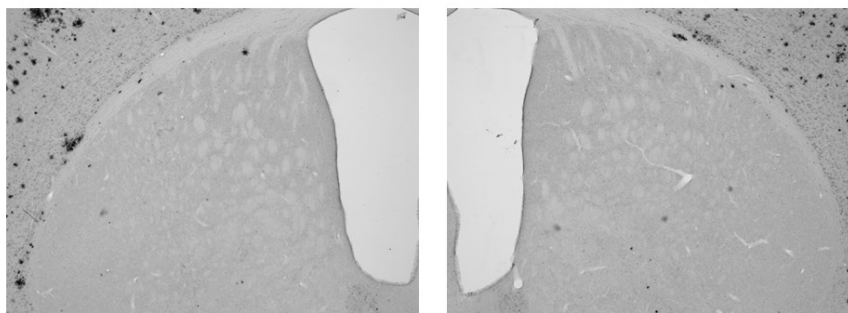
1. Pipette of the RNA phase
2. Add 500ul (1:1) 100% Ethanol to precipitate DNA and mix
3. Incubate for 5 minutes by 4°C
4. Centrifuge $7,500 \times g$ at 4°C for 5 min
5. Supernatent 1ml (phenol/ethanol fase) to a 2ml eppendorf tube for protein isolation
6. (Pellet can be used for gDNA isolation)
7. Add 1 mL (1:1) of isopropanol to the phenol-ethanol
8. Mix and Incubate for 10 minutes at RT
9. Centrifuge for 10 minutes at $12,000 \times g$ at 4°C to pellet the proteins
10. Discard the supernatant
11. Wash the pellet in 1.5 mL of wash solution (0.3 M guanidine hydrochloride in 95% ethanol)
12. Incubate for 20 minutes ad RT. (with shaking)
13. Centrifuge for 5 minutes at $7500 \times g$ at 4°C
14. Discard the supernatant. By poring

Supplementary table 1. Overview of all results. Summary of all significant results found in A β and synaptophysin expression. 0: no significant results, \uparrow : significant increase, \downarrow : significant decrease, $\uparrow\#$: trend which shows an increase, $\downarrow\#$: trend which shows a decrease.

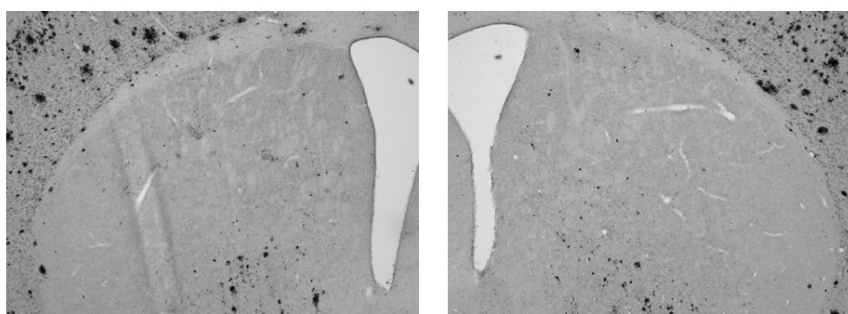
Target	Region	Parameter	Effect	Results
ELISA - A β	Anterior brain	A β 40	Right vs Left	0
			Stroke vs Sham	0
			Female vs Male	\uparrow in right and left hemisphere in female mice
		A β 42	Right vs Left	0
			Stroke vs Sham	0
			Female vs Male	0
		A β 42/ A β 40	Right vs Left	0
			Stroke vs Sham	0
			Female vs Male	0
IHC - A β 40	Cortex (-1.94)	Plaque size	Right vs Left	$\uparrow\#$ in male sham and female stroke mice
			Stroke vs Sham	0
			Female vs Male	0
		% +area	Right vs Left	0
			Stroke vs Sham	0
			Female vs Male	0
		#plaques/mm ²	Right vs Left	0
			Stroke vs Sham	0
			Female vs Male	0
	Hippocampus (-1.94)	Plaque size	Right vs Left	0
			Stroke vs Sham	0
			Female vs Male	0
		% +area	Right vs Left	\uparrow in female stroke mice
			Stroke vs Sham	0
			Female vs Male	\uparrow in left and right hemisphere in female mice
		#plaques/mm ²	Right vs Left	$\uparrow\#$ in female stroke mice
			Stroke vs Sham	0
			Female vs Male	\uparrow in left and right hemisphere in female mice
	Thalamus (-1.94)	Plaque size	Right vs Left	\uparrow in female sham mice
			Stroke vs Sham	0
			Female vs Male	\uparrow in right hemisphere in female mice
		% +area	Right vs Left	0
			Stroke vs Sham	0
			Female vs Male	\uparrow in left and right hemisphere in female mice
		#plaques/mm ²	Right vs Left	0
			Stroke vs Sham	0
			Female vs Male	\uparrow in left hemisphere in female mice
	Cortex (0.62)	Plaque size	Right vs Left	\downarrow in male stroke mice
			Stroke vs Sham	0
			Female vs Male	0
		% +area	Right vs Left	\downarrow in male stroke mice
			Stroke vs Sham	0
			Female vs Male	\uparrow in right hemisphere in female mice
		#plaques/mm ²	Right vs Left	\downarrow in male stroke mice
			Stroke vs Sham	0
			Female vs Male	\uparrow in left and right hemisphere in female mice
Corpus Callosum (0.62)	Plaque size	Right vs Left	0	
		Stroke vs Sham	0	
		Female vs Male	0	
	% +area	Right vs Left	0	
		Stroke vs Sham	0	
		Female vs Male	0	
	#plaques/mm ²	Right vs Left	\uparrow in male sham mice	
		Stroke vs Sham	0	
		Female vs Male	0	
Basal ganglia (0.62)	Plaque size	Right vs Left	0	
		Stroke vs Sham	$\downarrow\#$ in right hemisphere	
		Female vs Male	\uparrow in right hemisphere in female mice	
	% +area	Right vs Left	\downarrow in female stroke mice	
		Stroke vs Sham	0	
		Female vs Male	\uparrow in left and right (trend) hemisphere in female mice	

		#plaques/mm ²	Right vs Left	0
			Stroke vs Sham	0
			Female vs Male	↑ in left and right hemisphere in female mice
qPCR - SYP	Anterior brain	Synaptophysin	Right vs Left	↑ in male WT sham mice ↓ in female WT sham mice
			Stroke vs Sham	0
			Female vs Male	↓ in right hemisphere in WT sham mice ↓ in left hemisphere in APP mice
			APP vs WT	0

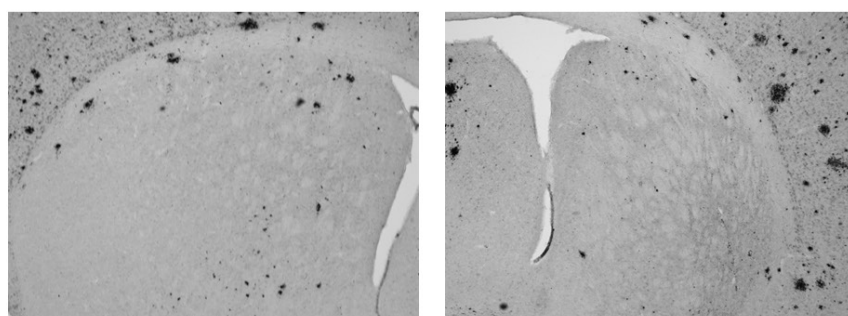
Male sham



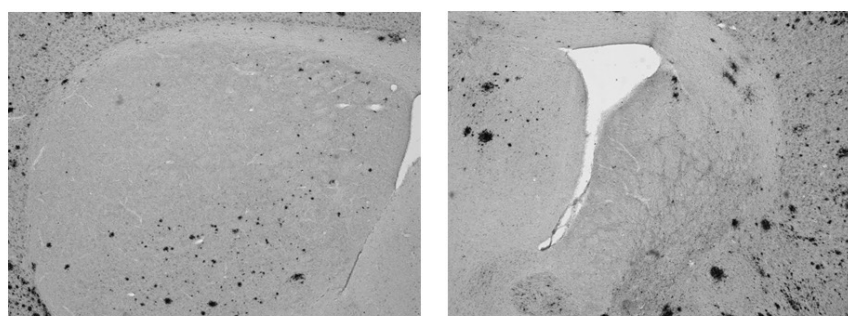
Female sham



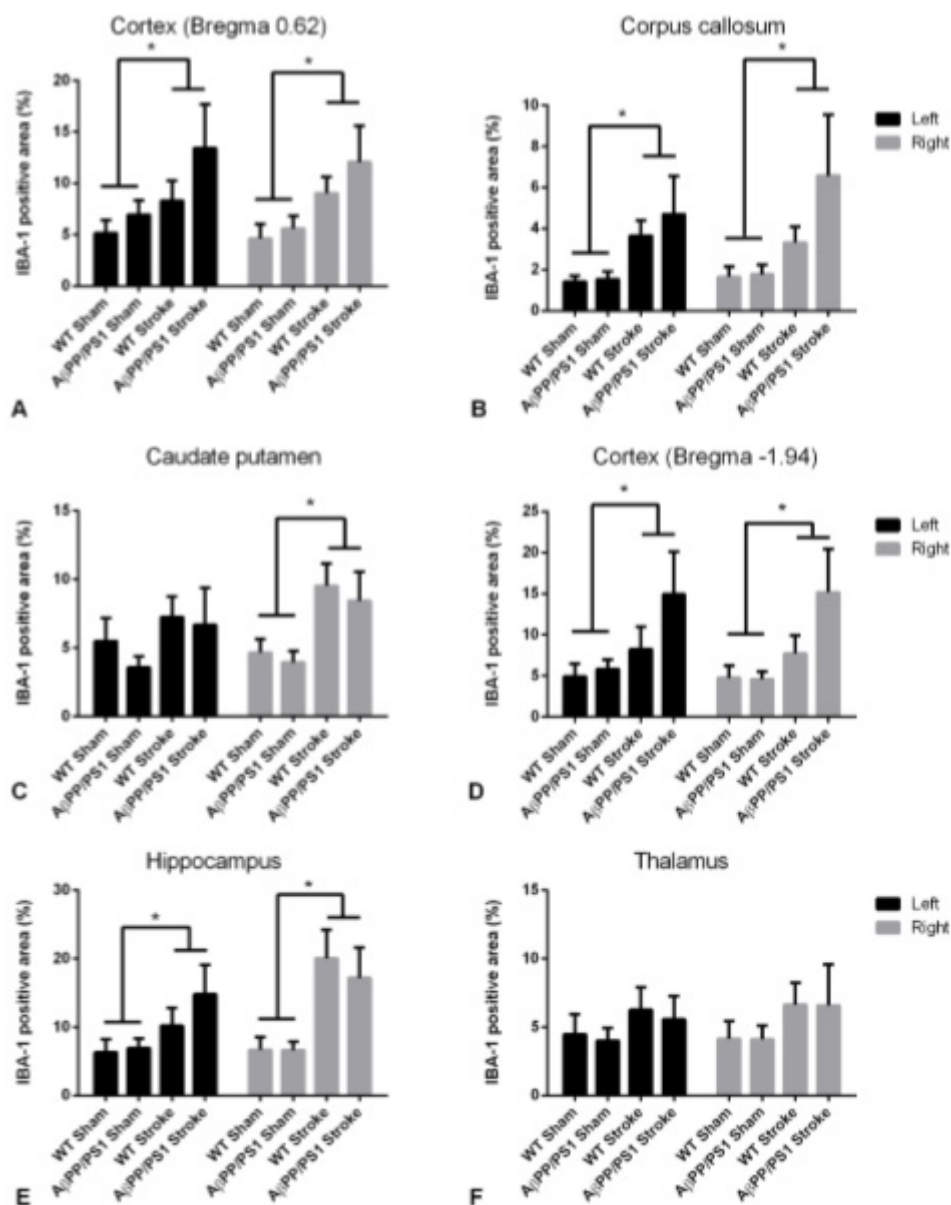
Male stroke



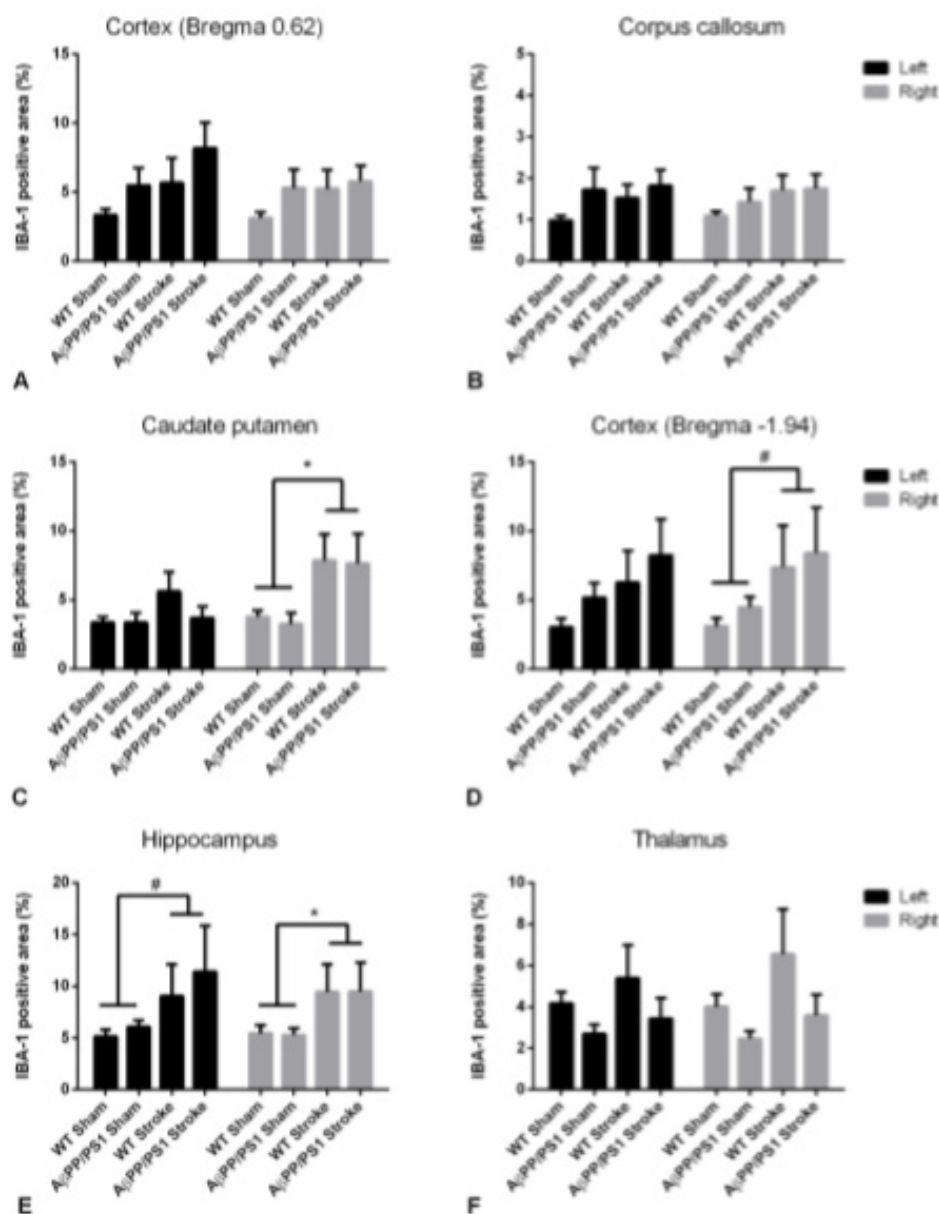
Female stroke



Supplementary figure 1. Atrophy in the basal ganglia. Representative photos of the left and right thalamus in male sham, female sham, male stroke and female stroke mice.



Supplementary figure 2. Neuroinflammation in male mice in the cortices, corpus callosum, caudate putamen, hippocampus and thalamus. All data are presented as mean \pm SEM. At bregma 0.62 the percentage of IBA-1 positive area was significantly increased in stroke mice compared to sham mice in the cortex in both the left ($p < 0.036$) and right ($p < 0.008$) hemisphere (A), in the corpus callosum in both the left ($p < 0.004$) and right ($p < 0.014$) hemisphere (B) and in the caudate putamen in the right hemisphere ($p < 0.003$) (C). The percentage of IBA-1 positive area was also significantly increased at bregma -1.94 in the cortex in both the left ($p < 0.027$) and right ($p < 0.010$) hemisphere (D) and the hippocampus in both the left ($p < 0.032$) and right ($p < 0.001$) hemispheres (E). No significant differences were found in the thalamus (F).



Supplementary figure 3. Neuroinflammation in female mice in the cortices, corpus callosum, caudate putamen, hippocampus and thalamus. All data are presented as mean \pm SEM. No significant differences in the percentage of IBA-1 positive area were found in the cortex (A) and corpus callosum (B) at bregma 0.62. The percentage of IBA-1 positive area was significantly increased in stroke mice compared to sham mice in the caudate putamen (C) in the right hemisphere ($p < 0.006$). A trend was visible in the cortex at bregma -1.94 (D) in which the stroke animals seemed to have an increased percentage of IBA-1 positive area compared to sham animals in the right hemisphere ($p < 0.077$). In the hippocampus (E) a trend was visible in the left hemisphere in which the stroke animals seemed to have an increased percentage of IBA-1 positive area compared to sham animals ($p < 0.078$). In the right hemisphere of the hippocampus, a significant increased in stroke mice compared to sham mice was found ($p < 0.047$). No significant differences were found in the thalamus (F).